Scientific Research Publishing

Oceans, Ice & Snow and CO₂ Rise, Swing and Seasonal Fluctuation

Michael D. Nelson[1], David B. Nelson[2]

[1]Retired Chemical Engineer and Patent Attorney, Pleasanton, USA
[2]Biology & Environmental Science, Granite Bay, USA
Email: mnelsonchemicalengineer@gmail.com

Abstract

Carbon dioxide rise, swing and spread (seasonal fluctuations) are addressed in this study. Actual CO₂ concentrations were used rather than dry values. The dry values are artificially higher because water vapor must be removed in order for the NDIR instrument to work and is not factored back into the reported numbers. Articles addressing these observations express opinions that are divergent and often conflicting. This investigation resolves many of those inconsistencies. The data were obtained from many measuring stations at various latitudes since 1972 and then graphical compared to changes in sea temperatures, fossil fuel emissions, humidity, and seasonal ice and snow changes. In analyzing the data, various parameters were addressed including: variability, R squared curve values, correlations between curves, residence times, absorption percentages, and Troposphere effects. Mass balance calculations were also made to corroborate viability. The CO₂ "rise" over a 33-year period from a slight ocean temperature increase (0.7˚F) contributed 2.3 percent of the total rise while fossil fuel emissions contributed 1.5 percent. The overwhelming majority (60 ppmv, 96%+) was caused by other factors including ocean and land biology as well potential errors in fundamental hypotheses. With respect to "spread" (seasonal CO₂ fluctuations) at the Polar Circles, graphical analysis with high correlations supported by mass balance calculations confirm that ice and snow are the primary cause and explain why the concentrations are the highest at these cold locations. The global variations in "swing" remain uncertain.

1. Introduction

Charles Keeling meticulously studied carbon dioxide variations from the Mauna Loa

Observatory in Hawaii and penned the famous "Keeling Curve". This curve formed the foundation for essentially all atmospheric CO_2 studies, both the yearly rise and the seasonal oscillations. Keeling unequivocally discovered that the average CO_2 concentration[1] has been rising over the last 100 years and that it fluctuates with the season with the Northern Hemisphere (NH) exhibiting the largest change.

There are three basic types of CO_2 observations. The "rise" is the most publicized and well known. It is the amount of CO_2 that increases every year. The monthly fluctuations or how the concentration changes with the seasons is the "spread". The third type is the "swing". It is similar to spread but measures the high and low differences between latitudes. Essentially, rise uses the same month and same latitude but different years; spread uses the same latitude and same year but different months; and swing uses the same month and same year but different latitudes.

The rise has been the subject of many scientific studies and forms the foundation for the global warming theory. Many believe that the "rise" is caused by burning fossil fuels [1] while others believe that increasing ocean temperatures may be responsible [2]. With respect to spread or seasonal fluctuations, the majority have placed the mechanism on bio-respiration of land plants in the Northern Hemisphere [3]-[6]. These studies point to the Northern Hemisphere because it covers 70% of the earth's land mass and therefore contains more land plants. Some studies have opined that the rain forests in the Southern Hemisphere (SH) were CO_2 neutral, *i.e.* the absorption of CO_2 by the plants was offset by the simultaneous decay of vegetation, thus explaining the lesser fluctuations in the SH.

Other scientific papers postulate that the yearly spread or seasonal oscillations are caused by a combination of fossil fuel emissions and bio respiration as moderated by a stronger than expected NH sink [7]. Northern soil respiration may play a significant part [8] [9]. The Arctic tundra may act as a summer CO_2 sink [10]. A combination of bio-respiration, precipitation, and circulation has been investigated [11]. An inverse relationship with the Southern Oscillation Index has been reported [12]. A combination of volcanic eruptions, El Nino and NAO (North Atlantic Oscillation) has been explored [13]. A connection between the Southern Annual Mode (SAM) and El Nino may exist [14]. One study reported a combination of everything, *i.e.* changes in mean air and sea temperatures, upwelling of CO_2 rich ocean waters, terrestrial ecosystems, El Ninos, and soil moisture changes [15]. Connecting ocean carbon cycles to APO (oxygen + CO_2) appears to have a significant relationship [16].

Scientific studies of the "swing" are typically discussed as subsets of rise or spread investigations.

The IPCC (Intergovernmental Panel on Climate Change, a division of the UN) lists the largest atmospheric CO_2 exchanges, *i.e.* the total of emissions (sources) and absorptions (sinks). Included in this list are oceans at 182 GtC/yr, land plant biology at 102 GtC/yr and land soils at 100 GtC/yr. Fossil Fuel emissions sit at 5 GtC/yr. [1] Hence, oceans, biology, and soils constitute 97% of all sources/sinks.

---

[1]Concentration is technically not the correct term. However, because so many publications use concentration to mean volume ratio (volume of CO_2 to volume of air), that will be the definition used herein.

There is a close inverse relationship between seasonal changes in sea temperatures and seasonal changes in the carbon dioxide concentrations. That is, when sea temperatures fall the atmospheric CO_2 concentration increases, and when temperatures increase CO_2 goes down. The same inverse relationship occurs with air temperature, *i.e.* a rising temperature and a falling CO_2. Some scientists used the inverse land/air temperature relationship as a proxy for a biological connection, *i.e.* as the temperature goes up, land plants grow and consume CO_2 by photosynthesis (sink).

None of these studies have adequately answered the question as to why the North and South Polar Regions each have the highest CO_2 concentration, or how a lack of land bio-masses within 1000 kilometers of either pole could cause such a high concentration. This study addresses all three types of observations: rise, swing and spread, as well as the potential causes for each. It also provides an explanation for why these cold regions record the highest CO_2 concentrations.

2. Issues Relating to CO_2 Data

2.1. How CO_2 Is Measured

According to the NOAA's (National Oceanic and Atmospheric Administration, a division of the US Department of Commerce) description of the laboratory test [17], a flask containing the air sample is passed through a water trap maintained at about −70 degrees C. This freezes out most of the water vapor. The dry sample is then passed through a non dispersive infrared (NDIR) analyzer. The analyzer exposes the sample to infrared radiation and a detector measures the absorption profile and strength of the ensuing signal. The results are then compared with the signals from two different calibrated reference gases having known CO_2 concentrations that bracket the expected concentration. The sample gas concentration is then calculated. The NDIR only works if all the water vapor is removed since the absorption spectra of water will affect the results.

The CO_2 test procedure reports an artificial or dry concentration—not the actual concentration. Since the water vaper in the air can constitute about 3% of the air in equatorial waters, removing it increases the dry CO_2 concentration by 12 to 15 ppm. This is because a cubic meter of any gas contains the same number of molecules (Avogadro's number) at the same temperature and pressure regardless of the kind of molecules present. If 3 percent of water molecules are added or removed, it will change the percentage of the other gases by the same ratio, *i.e.* 3 percent. The equatorial regions contain a significant amount of water vapor while the Polar Regions contain very little. In these colder regions the removal of the water has very little effect on the actual CO_2 concentration.

The explanation for reporting the dry CO_2 concentration and not the actual CO_2 concentration is that humidity varies between day and night and between high and low altitudes. This would result in a variable concentration and make comparisons difficult. In addition, if the CO_2 data are reported as anomalies (comparative change) then the anomalies in the dry CO_2 concentration would be very close to the anomalies in the actual CO_2 concentrations. That is, the **change** (anomaly) in the dry CO_2 concentration

from the previous day, month or year would be very similar to the **change** (anomaly) in the actual CO_2 concentration from the same previous day, month or year. Both of these explanations are technically correct. However, just because something is difficult to accurately track does not mean that there is a valid reason to disregard it.

Plots of dry CO_2 anomalies compared with actual CO_2 anomalies show that the two are indeed exceptionally close. Therefore if anomalies are the only thing being considered, then there is a valid reason for using dry CO_2 concentrations as a proxy for actual CO_2 concentrations.

Scientists have become so accustomed to the "Keeling Curve", that many have missed the distinction between dry and actual. This can result in some errors and confusion.

A particular problem occurs with entropy. At the Poles, the dry CO_2 concentration is essentially equal to the actual concentrations. But with each drop in latitude, there is a corresponding increase in water vapor, and the difference between dry and actual becomes higher and higher. This difference ranges from 0 - 2 ppm in the Polar Regions and increases to 13 - 15 ppm at the equatorial regions. With respect to entropy, this is a significant issue. For example, in August 2014 the North Pole (Alert 82˚N) had a dry CO_2 concentration of approximately 389 ppmv. At the equator (Christmas Island 1.87˚N) for the same time the dry concentration was 397 ppm. This suggests an August mass flow driving force (Δ8 ppm) toward the North Pole. It further infers that CO_2 may be accumulating in the lower latitudes; and some have suggested that it is the result of fossil fuel burning. But the actual CO_2 concentration at Christmas Island was 382 and not 397. This shows that the mass flow driving force is in the opposite direction—from the North Pole to the equator and does not support an equatorial accumulation.

2.2. Atmospheric Water Vapor

Actual CO_2 concentrations can be calculated at the time of sampling by measuring the temperature and relative humidity. Humidity measurements can also be ascertained during laboratory testing by recording the amount of water in the water trap per unit of sample volume.

Unfortunately, neither of these humidity measurements were reported. The humidity can be estimated by determining the average humidity at a location near the CO_2 sampling station. Figure 1 shows how the average sea level humidity varied with latitude and month. This figure illustrates that the water vapor (specific humidity) varied from near zero at the polar regions to a maximum of 330,000 ppmv at the equator. It shows that the Northern Hemisphere is more variable[2] than the Southern Hemisphere.

Figure 1 illustrates significant variability around 30 degrees, particularly in the North. Thirty degrees is one of the important latitudes regarding atmospheric wind patterns. This is a transition zone between the westerly polar winds and the easterly equatorial winds. It is here that the Handley Cell circulates vertical winds rising from the humid equatorial regions and returning to the surface near 30 degrees. This may

---

[2]The humidity measurements in this study were located near ocean sources and do not reflect humidity over land areas. The humidity at the South Pole was calculated because of the extremely low temperatures. Variability means simply a difference in values from a norm value.
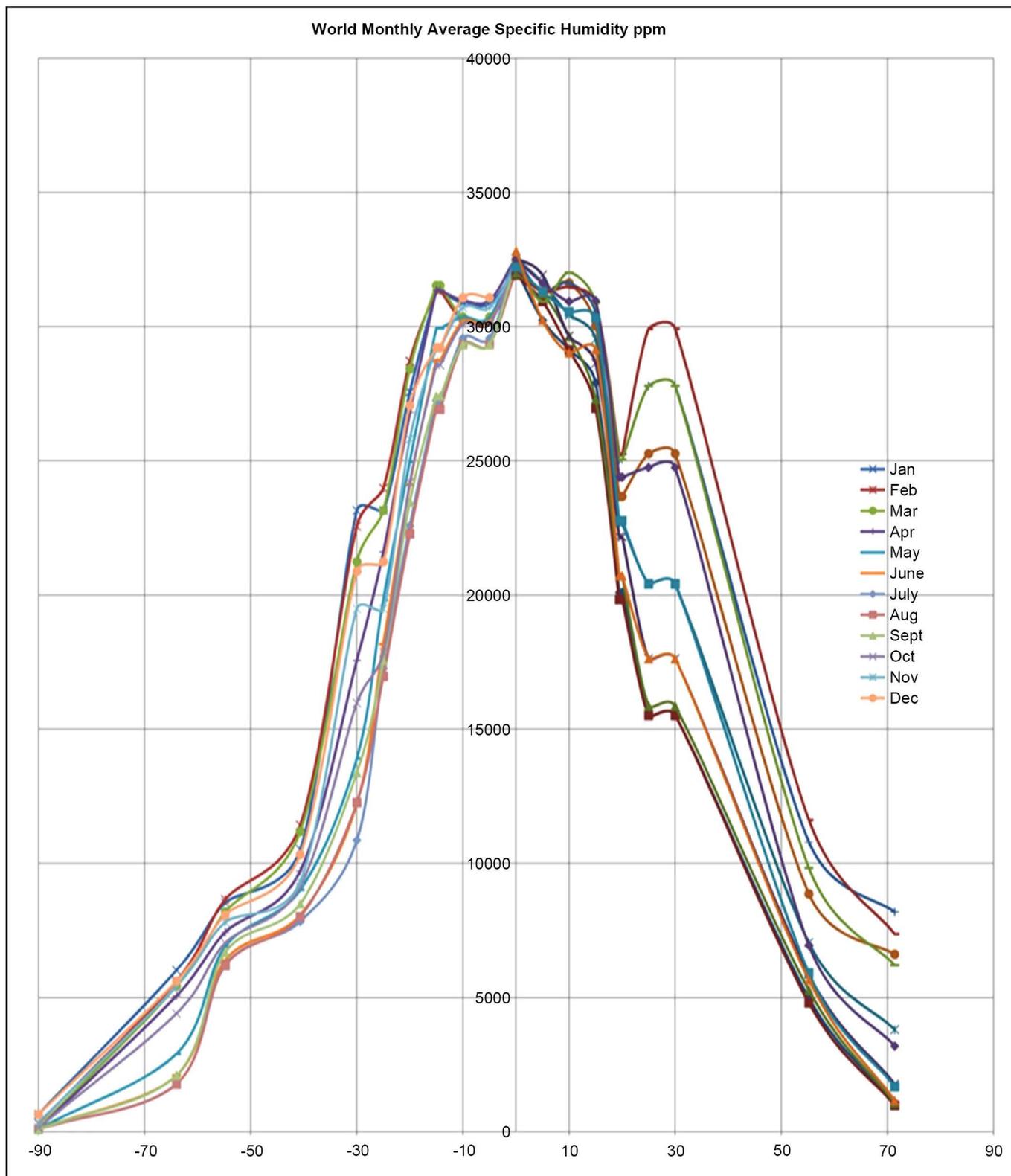
Figure 1. Plots the average specific humidity converted to ppmv of the air at various latitudes. Specific Humidity was calculated from Relative Humidity and temperature data obtained from Weather 2 Ltd Glasgow, UK, and Weather-and-Climate by World Wide Travel Organization, Netherlands.

explain the spike in humidity at 30 degrees. There is an inverse spike of CO_2 near 30 degrees, *i.e.* a dip in CO_2 that mirrors the increase in specific humidity. Like sea and air temperatures, the inverse relationship between atmospheric CO_2 and ocean humidity is consistent and its cause uncertain.

In this investigation the average specific humidity at each measuring station was used. It is recognized that using averages is less accurate than using actual numbers. The average humidity does not reflect that the water vapor content has been rising each year [18]. Between 1971 and 2013 the ocean humidity anomaly increased approximately 0.4 grams of water per Kg of air. As such, it is likely that actual CO_2 numbers calculated in this study will be lower than those reported. That is, the dry CO_2 numbers are likely more overstated than shown here.

One study [18] reported that the average land specific humidity **anomaly** was similar to the ocean **anomaly**. Using anomalies can be misleading since the changes in actual specific humidity can be many times greater over land as compared to the ocean. The difference in ocean specific humidity is relatively narrow and follows a predictable pattern, *i.e.* a declining humidity with latitude. On the other hand, the specific humidity over land is entirely different. It can go from near zero to 30,000 ppmv at the same latitude. For example, the anomaly for the Atacama Desert and the Brazilian rain forest may each be near zero. Some may deduce from a zero anomaly at both locations that each may have a similar humidity. In reality they can be 30,000 ppmv apart. This does not mean that anomalies are not useful or are invalid. It only means that comparing anomalies with actual concentrations/temperatures/pressures etc. can be a source of confusion.

2.3. CO_2 Dry-Actual Comparison

In the Polar Regions the dry CO_2 and the actual CO_2 concentrations are nearly the same. This is illustrated by **Figure 2** plotting the two measurements from Barrows Alaska (71˚N). All dry CO_2 data was obtained from the Earth Systems Research Laboratory of the National Oceanic & Atmospheric Administration (NOAA). All references to ESRL are from this data source. The selected year is representative since graphs for different years show the same type of relationship.

Figure 3 is the same type of graph except using data from Christmas Island (1.87˚N), which is representative of the equator. Comparing **Figure 2** and **Figure 3** shows an increasing deviation associated with a drop in latitude. The deviations between dry and actual in the Southern Hemisphere are similar.

Figure 3 shows that the two curves are relatively flat near the equator as compared to differences at the northern latitudes. The general shape of the curves is similar at different latitudes except for a declining difference in dry/actual ratio in the north and a flip between the hemispheres because of the reversal of summer to winter. The curve shape near the equator is more erratic because of the clash of the two hemispheric atmospheres transitioning into each other.

Figure 4 is a plot of the dry CO_2 anomaly in 2012 compared to 2011 with the actual CO_2 anomaly for the same period at Christmas Island, Kiribati. Comparing **Figure 3**
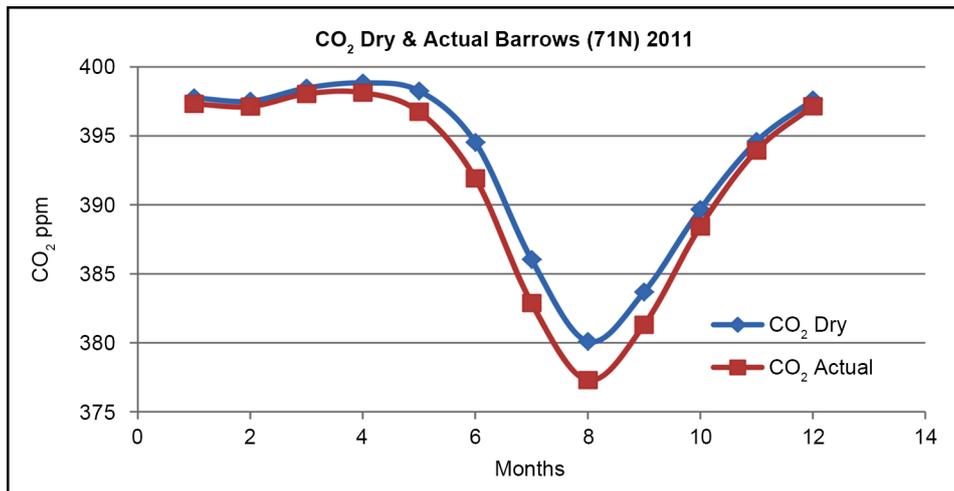
Figure 2. Is a plot of monthly CO_2 concentration (ppmv) from Barrows, Alaska in 2011. The dry CO_2 data set was from ESRL. The actual CO_2 data was calculated from the dry data by applying an average humidity factor.
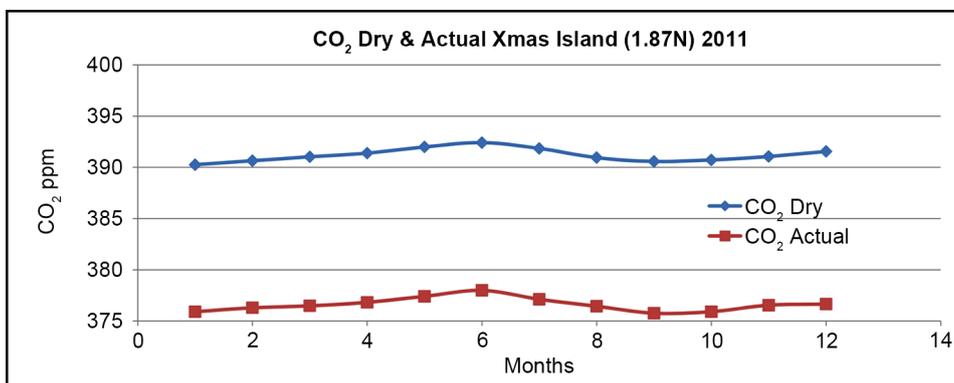

Figure 3. Is a plot of monthly CO_2 concentration (ppmv) from Christmas Island (1.87˚N) in 2011. The dry CO_2 data set was from ESRL.
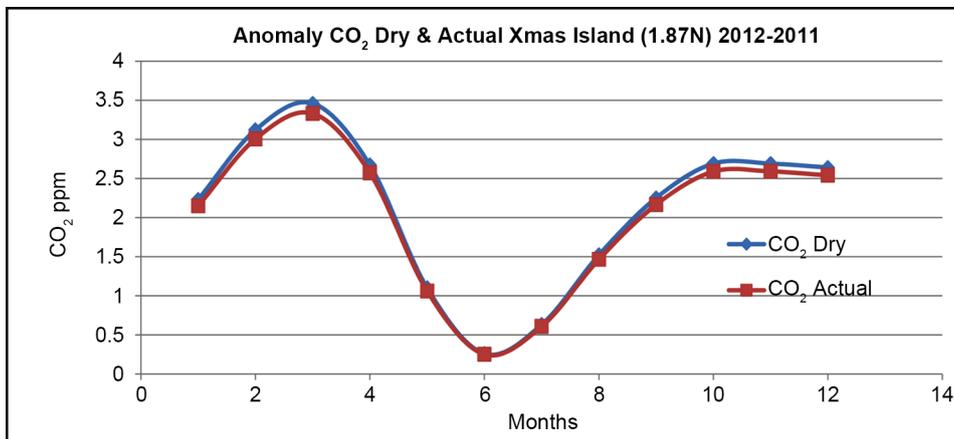

Figure 4. A comparison of the CO_2 dry monthly anomaly between 2011 and 2012 with CO_2 actual monthly anomaly over the same period for Christmas Island (1.87˚N) The dry CO2 data was from ESRL. Note the difference from **Figure 3**.

with Figure 4 at the same location and at the same time illustrates how anomalies can be misleading. On the other hand, it shows that a dry CO_2 anomaly can act as a good proxy for the actual CO_2 anomaly depending on how the reference date is selected.

In summary, the actual CO_2 concentrations are similar to the dry concentrations but shifted downward. The amount of downward shift increases with decreasing latitudes in both hemispheres. The use of anomalies masks the downward shift.

3. CO₂ Rise, Swing, and Spread (Seasonal Fluctuation)

3.1. Concentration Profiles

All of the figures and tables shown/discussed hereinafter are based on actual CO_2 concentrations and not dry concentrations unless otherwise indicated. Figure 5 is a CO_2 plot for 2011 broken down by month for each station at various latitude spanning the South Pole (−90˚S) to Barrows, Alaska (71˚N). Although 2011 was selected, it is representative of the other years. The most significant change between years is that the CO_2 concentration has been rising.

The 2011 monthly variations in the Northern Hemisphere (NH) were more erratic than those in the Southern Hemisphere (SH). At −90˚S the spread was about 2.5 ppmv with fluctuations grouped into three 4-month segments. That is, the high concentrations lasted about 4 months, the lows for 4 months, and the transitions at 4 months. The NH had a spread at Barrows almost 8 times greater at 20 ppmv. The highs lasted 6 months, the low lasted 1 month, and the transitions spanned 5 months.

The NH comparison is different from the SH in that Barrows, Alaska is located at 71˚N and not 90˚N, and requires a latitude adjustment. There were some differences with the 2011 observations between latitudes, particularly around 30 degrees. The spread in the Southern Hemisphere (SH) ranged from about 0.8 ppmv at the equator to 4.5 ppmv at −30˚S whereas the spread in the Northern Hemisphere (NH) ranged from 0.8 at the equator to 20.8 ppmv at Barrows, Alaska. The observed spreads were many times larger in the north.

The 2011 swings were also different. The minimum swing occurred in February-March in the SH at about 8.4 ppmv. In the north, the minimum swing was 8 times less occurring in August at 1 ppmv. The maximum swing occurred in October in the SH at about 11 ppmv while it occurred in April in the NH at 19.8 ppmv. In the SH the driving force (delta concentration) varied from ~11 ppmv (Oct) to ~8.4 ppmv (March). The NH, on the other hand, had a driving force of 19.8 ppmv (April) to 1 ppm (Aug). This shows a maximum difference in push-pull force of 19 ppmv in the north and 2.7 ppmv in the south.

Figure 6 illustrates these driving forces in terms of vectors for the Northern Hemisphere. A similar graph for the SH is not presented since there were minor changes in the vectors. This figure illustrates a one year mass flow analysis with flow vectors favoring a downward direction.

The vectors were additive (accelerates flow) anytime there were decreasing CO_2 concentrations, and subtractive, (inhibits flow) during times of increasing concentration.
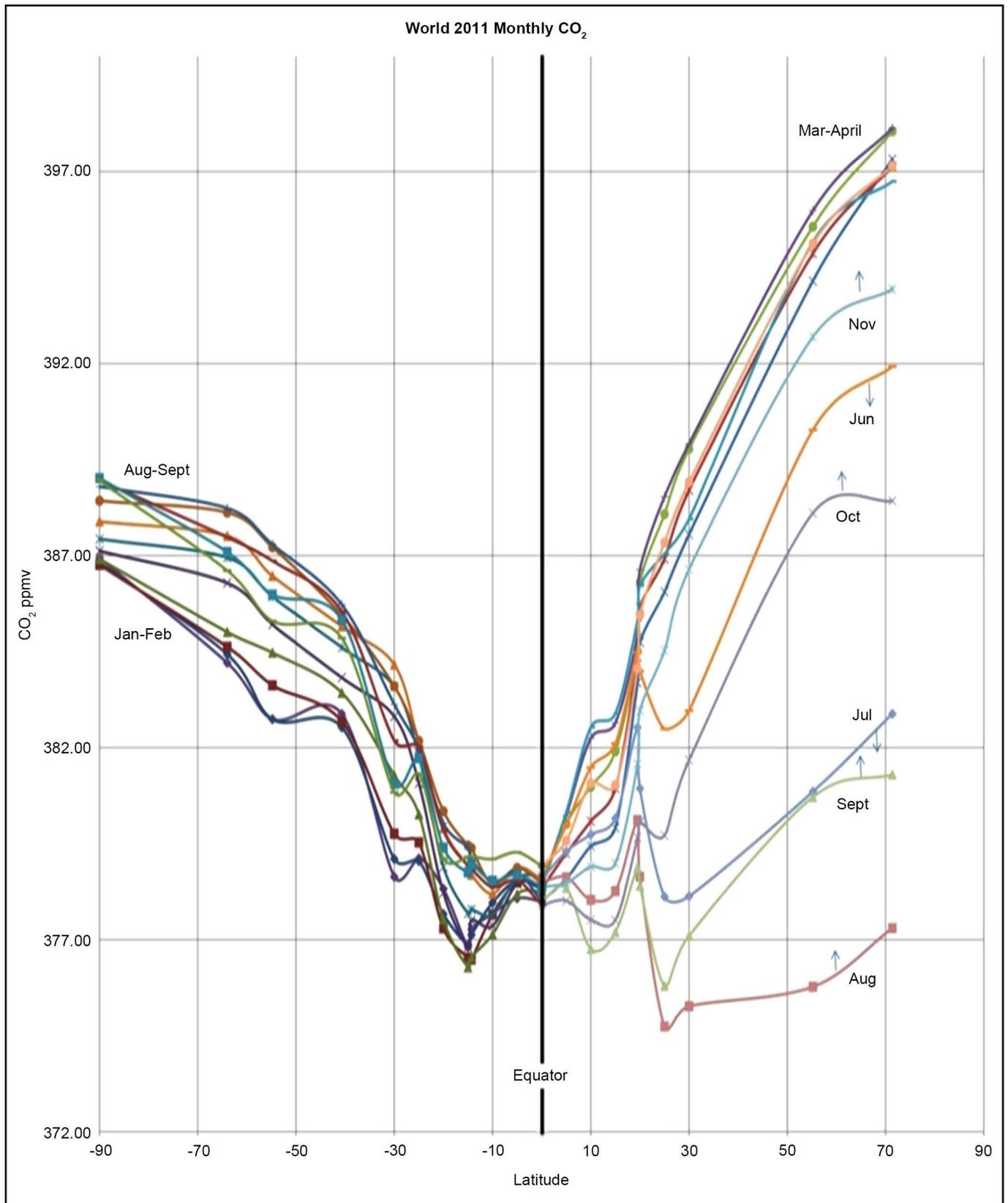
Figure 5. A plot of actual monthly CO₂ concentration with latitude for 2011.
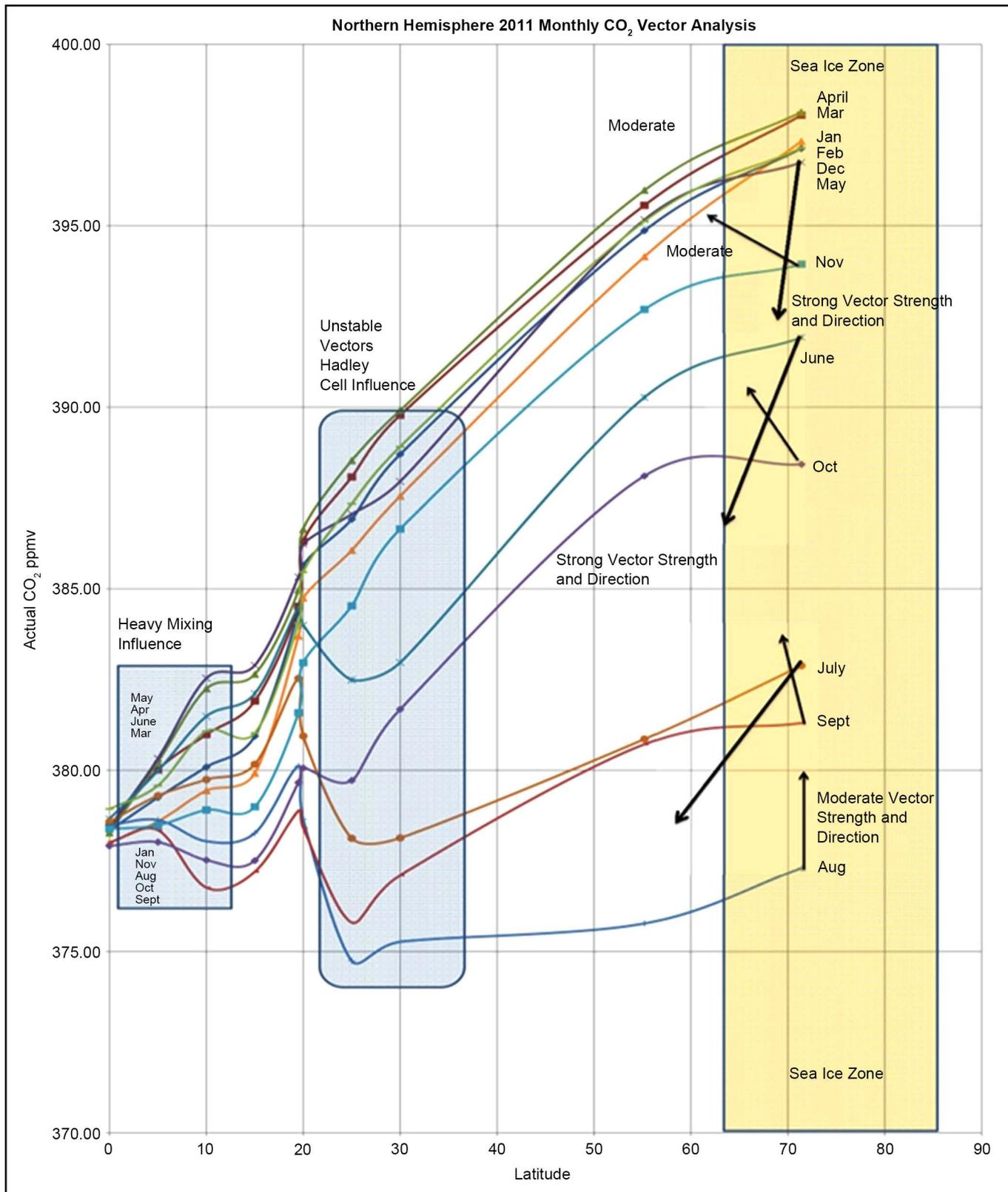
Figure 6. A vector analysis of the actual monthly CO_2 concentration with latitude in the Northern Hemi-sphere for the year 2011. Length of vector connotes strength and the arrow connotes direction.

This is illustrated in the above graph when the concentration was dropping, *i.e.* May and August it took 3 months to complete the drop. When the concentration was increasing, *i.e.* September to December it took 3.5 months to accomplish the same spread. The lower CO_2 concentrations from lower latitudes likely rob (inhibit) a portion of the CO_2 from building at the higher latitudes between Sept to Dec thereby slowing the accretion and adding (assists) in the other direction. There are other one-year cyclic systems that may have a faster rise/drop direction and could be additional factors in explaining the observations. It is possible that ice melts or freezes more quickly in one direction than the other. The heat of fusion (freezing/melting) traveling into a point may be different from heat radiating outward. It is possible that sea temperatures rise or fall faster in one direction. Perhaps the ozone layer is preferentially weaker or stronger during the year and this process affects temperatures, ice formation or melting, soil desiccation, and/or CO_2 absorption/ejection. Or it may be a combination of all of these factors and others.

Whatever the actual causes, the mathematical vector analysis assists engineers in exploring the potential causes and effects.

3.2. Rise, Swing & Spread

The CO_2 concentration profiles displayed in Figure 7 & Figure 8 illustrate changes in the rise and swing. Second order polynomial equations were the best fit to describe the curve for the rise, while a linear curve was used to describe the swing. The equations were not set forth on the graph because "years" were used in the X axis. Years are large numbers and when multiplied or squared, it makes the coefficients in front of the X variable extremely sensitive, requiring very long numbers, *i.e.* up to 10 decimal places.

3.2.1. Northern Hemisphere

The January rise plotted in Figure 7 for the NH showed that an upper border occurred at 71˚N degrees (Barrows, Alaska) and 82˚N degrees (Alert, Canada), a bottom border occurred at 1.87˚N degrees (Christmas Island) and all other latitudes were bracketed. The upper border had a rise of 51.67 ppmv between 1986 and 2014 illustrating an average yearly rise of 1.84 ppmv. The bottom border raised 48.4 ppmv between those years with a yearly rise of 1.72 ppm/yr. Although there was data going back to 1975 for the upper border, the bottom border only had data going back to 1985. There were differences between the months as illustrated in Figure 5, but the relative rise was similar, *i.e.* the August rise was 49.5 ppmv (Christmas Island) and 48.6 ppmv (Alert). A gap in the curves between 30˚N degrees and 55˚N degrees can be seen and may be associated with the Hadley Cell.

The January swing exhibited ~16 ppmv in 1986 that increased to ~20 ppmv in 2014. The swing increased about 4 ppmv in 28 years or 0.14 ppmv/yr. The swings varied greatly (1 - 20 ppmv) between months in the NH as shown in Figure 5. These swings increased about 17.5% between 1986-2014 as shown in Figure 9. In the SH., the monthly swings were considerably less varied (8.4 - 11 ppmv) as shown in Figure 5, and had a near zero change between years (Figure 9).
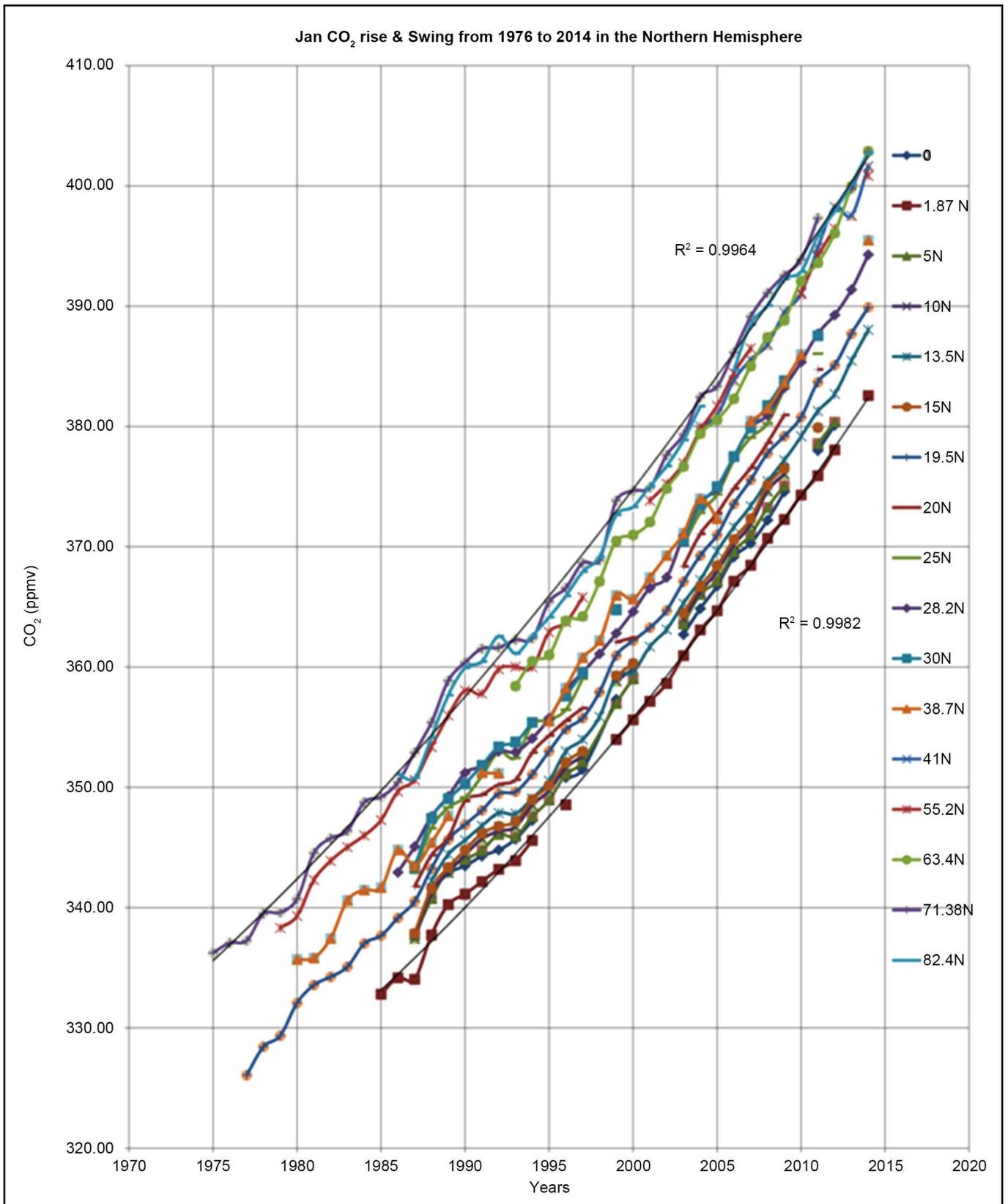
Figure 7. Rise & Swing in January CO_2 for Northern Hemisphere between 1976-2014. The dry CO_2 data set was from ESRL.
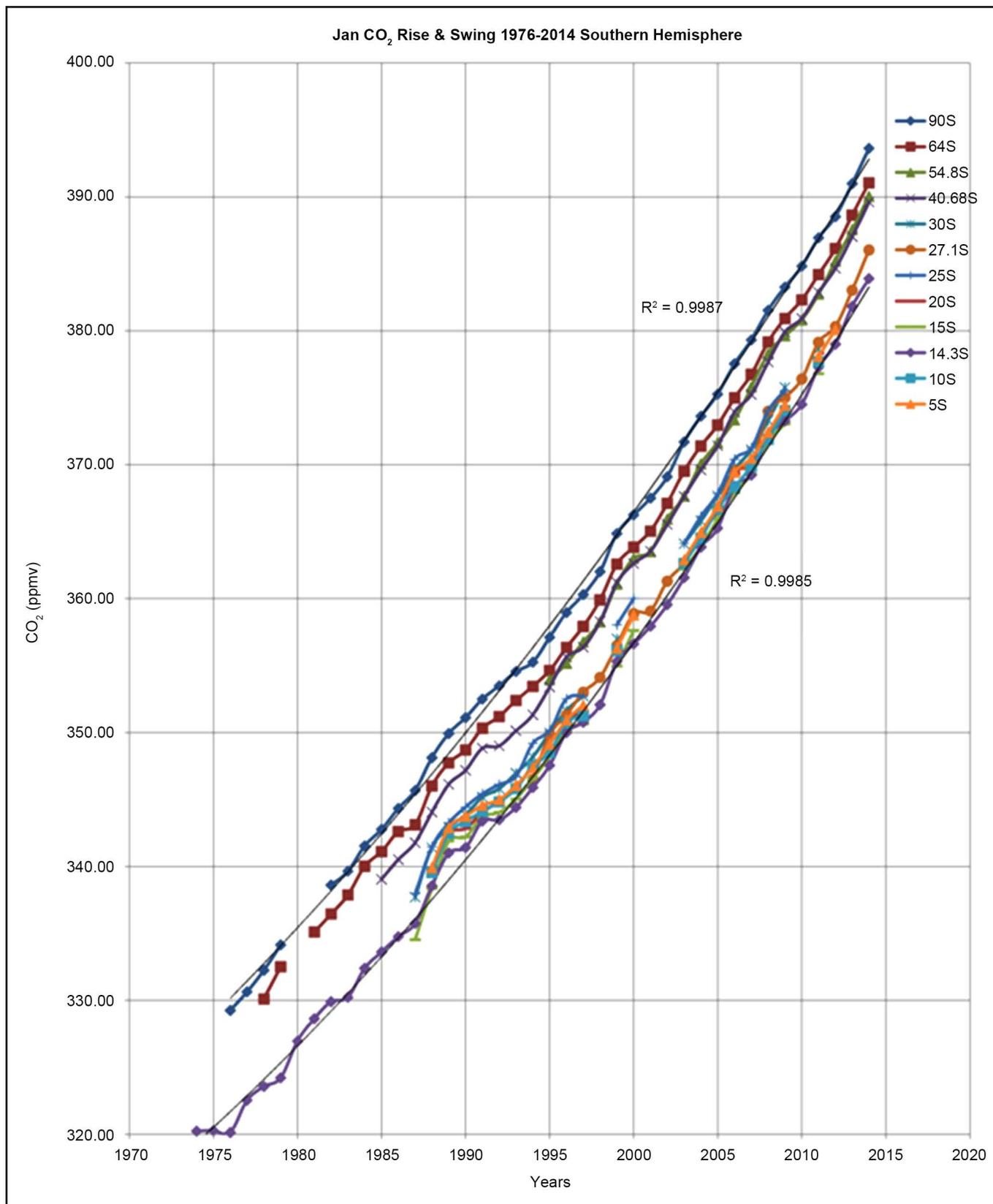
Figure 8. Rise & Swing in January CO_2 for Southern Hemisphere between 1976-2014. The dry CO_2 data set was from ESRL.
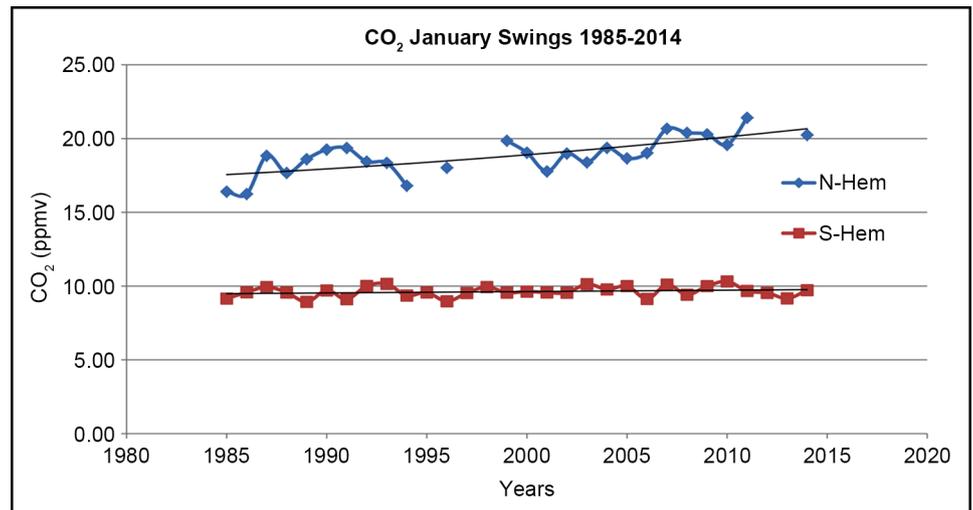
Figure 9. Plot of January CO_2 Swing Concentrations between 1985 and 2014 in both the Northern and Southern Hemispheres.

The spread is not shown in Figure 7 & Figure 8.

3.2.2. Southern Hemisphere

The January rise plotted in Figure 8 showed that an upper border occurred at the South Pole (−90˚S), a bottom border at Samoa (−14.3˚S), and bracketed the rise in all other latitudes. The upper border had a total rise of 64 ppmv between 1976 and 2014 (38 years).This represented an average yearly rise of 1.68 ppmv/yr. This was slightly lower than the rise observed in the NH. The bottom border has a rise of 64 ppmv between those years yielding the same average yearly rise of 1.68 ppm/year.

Figure 8 illustrates that the swings were constant between the years, *i.e.* the upper border and the lower border were basically parallel. Like the NH, there was an interesting gap between −28S degrees and −40S degrees that may be associated with the Hadley Cell. The SH January swing between 1986 and 2014 varied from 9.57 to 9.72. The swing data showed a minor increase of 0.15 ppmv during this period.

Figure 9 illustrates the changes in the January CO_2 swings from 1985 to 2014. The latitudes giving the largest swings were Barrows, Alaska to Christmas Island in the Northern Hemisphere and the South Pole to Samoa in the Southern Hemisphere. There were noticeable swing deviations in the NH with fewer deviations in the SH. Each curve had high variability and exhibited an R squared value less than 50%.

The following Table 1 sets forth the changes both in ppmv and in percentages for the spread and rise in both hemispheres. The rise percentage over the last 28 years (varied with available station data) averaged 0.473% for the SH and 0.461% in the NH. The spread percentage averaged 0.93% for the SH and 3.4% for the NH. The average CO_2 concentration ranged from 358 to 376 in the NH and ranged from 356 to 371 in the SH.

The swings were not presented in the Table because they are high and low comparisons between latitudes.

There may be some discrepancies between Figure 7 & Figure 8 and Table 1. The table

Table 1. Changes in the Jan rise and highest spread of CO_2 at various latitudes. The percentages are computed by dividing the spread or rise ppmv by the average CO_2 concentration for February in NH and April in SH.

Station	Lat.	Ave CO₂ (ppmv)	Max Spread (ppmv)	Max Spread (Percent)	Ave Rise/yr (ppmv)	Ave Rise/yr (Percent)
South Pole	−90˚S	369	3.02	0.81%	1.66	0.45%
Palmer Station	−64˚S	365	3.68	1.00%	1.69	0.46%
Ushuaia, Argentina	−54.8˚S	371	4.12	1.11%	1.79	0.48%
Cape Grim	−41˚S	363	3.51	0.96%	1.68	0.46%
Pacific Ocean	−30˚S	358	4.08	1.14%	1.57	0.44%
Easter Island	−27˚S	366	4.49	1.23%	1.86	0.51%
Pacific Ocean	−25˚S	357	3.95	1.11%	1.66	0.46%
Pacific Ocean	−20˚S	356	2.75	0.77%	1.64	0.46%
Somoa	−14.3˚S	358	3.01	0.84%	1.55	0.43%
Pacific Ocean	−10˚S	357	1.32	0.37%	1.59	0.44%
Pacific Ocean	0˚	359	1.37	0.38%	1.5	0.41%
Christmas Island	1.87˚N	358	2.28	0.63%	1.64	0.46%
Pacific Ocean	10˚N	360	6	1.67%	1.73	0.48%
Barbados	13.1˚N	365	7.29	1.99%	1.69	0.47%
Pacific Ocean	15˚N	360	6.19	1.71%	1.66	0.46%
Mauna Loa	19.5˚N	365	6.22	1.7%	1.69	0.46%
Pacific Ocean	25˚N	366	15.1	4.1%	1.68	0.45%
Midway	28.2˚N	368	14.1	3.8%	1.75	0.47%
Azores	38.7˚N	368	16	4.4%	1.70	0.46%
Cold Bay, Alaska	55.2˚N	373	20.2	5.4%	1.7	0.46%
Barrows, Alaska	71.3˚N	376	20.8	5.5%	1.6	0.43%
Alert, Canada	82.4˚N	376	20.193	5.4%	1.77	0.47%

uses a larger number of sampling stations than the figures, but many of the sampling stations did not have data going back to 1976.

Figures 10-16 graph the rise and spread changes in terms of percent. The February data were used to compute the rise for the SH and the April data was used in the NH. The yearly rise for all latitudes showed a similar slope. With respect to spread, the maximum and minimum months of October & February (winter-summer) were used for the Southern Hemisphere and April & August (winter-summer) were used for the Northern Hemisphere.

Figure 10 plots the rise and spread from 1986 to 2014 at the South Pole (−90˚S).
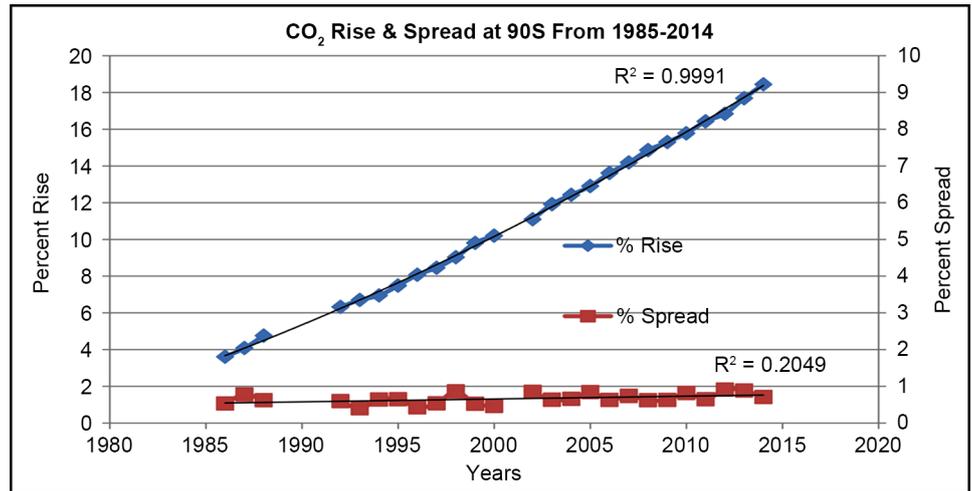
Figure 10. A graph of the percent rise & spread in actual CO_2 at the South Pole (−90˚S).
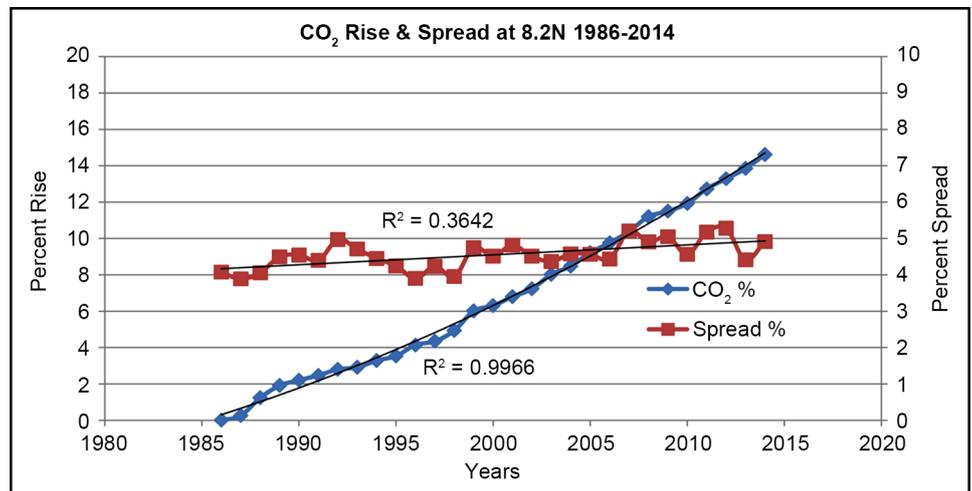

Figure 11. A graph of the percent rise & spread in actual CO_2 near the North Pole at Alert (82.4˚N).
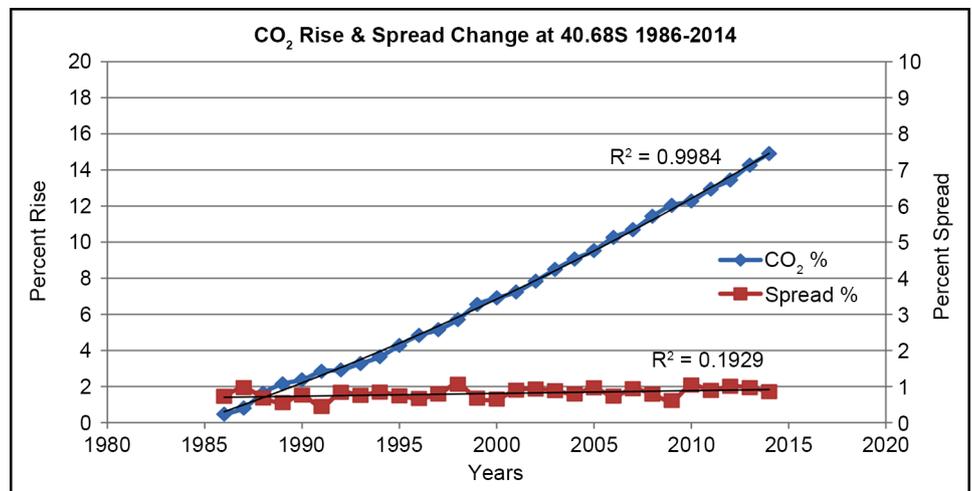

Figure 12. A graph of the percent rise & spread in actual CO_2 at Cape Grim (−41˚S).
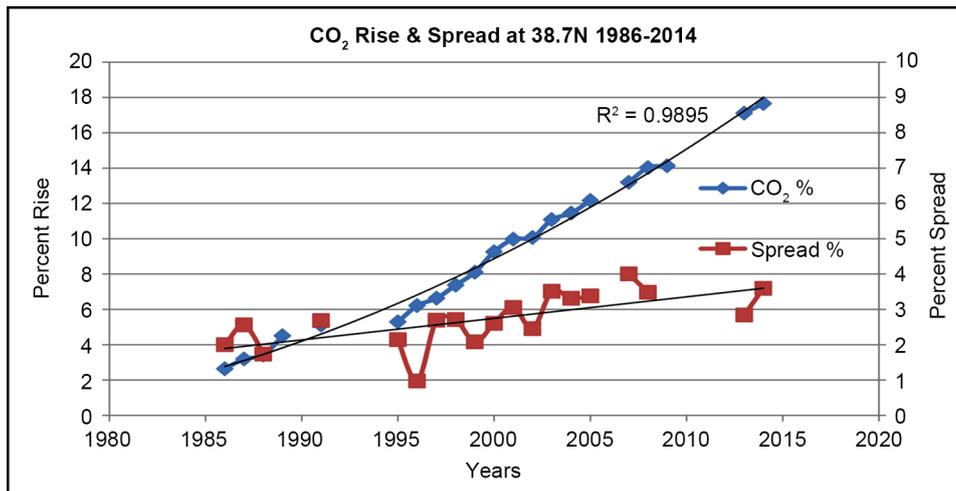
Figure 13. A graph of the percent rise & spread in actual CO_2 at Azores (38.7˚N).
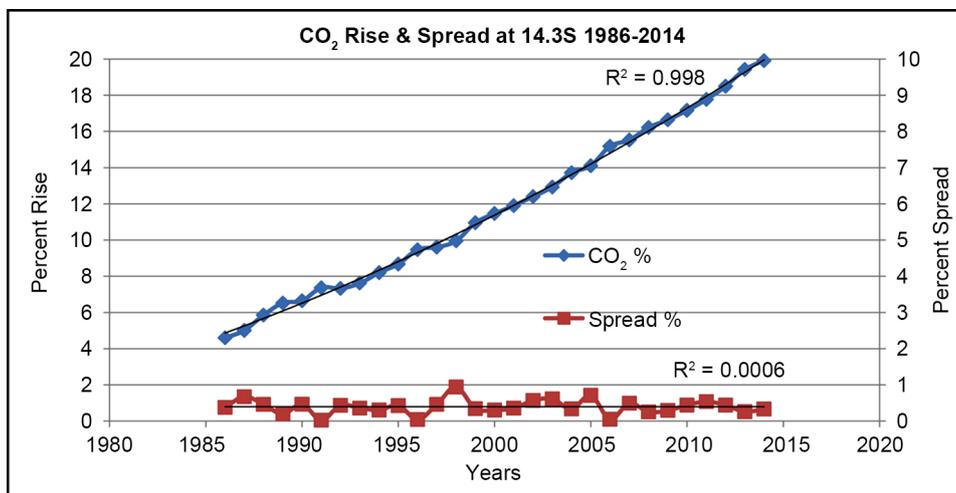

Figure 14. A graph of the percent rise & spread in actual CO_2 at Samoa (−14˚S).
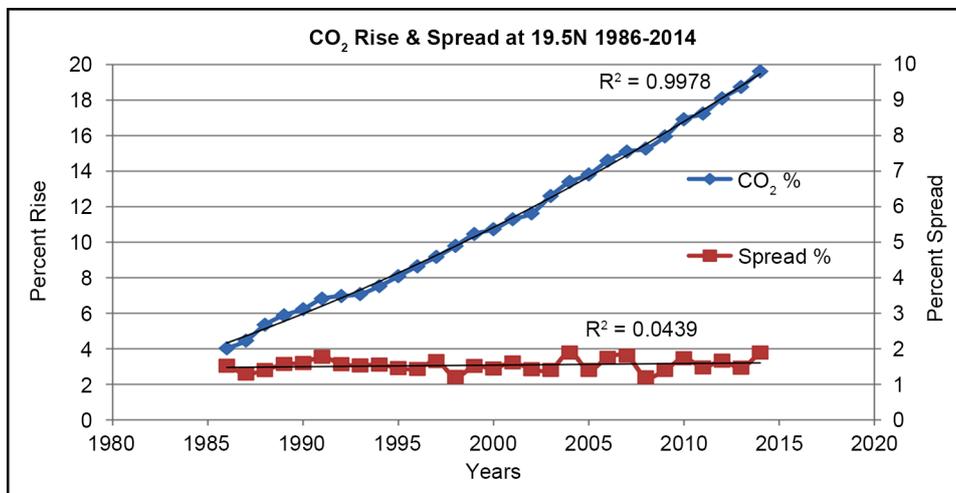

Figure 15. A graph of the percent rise & spread in actual CO_2 at Mauna Loa (19.5˚N).
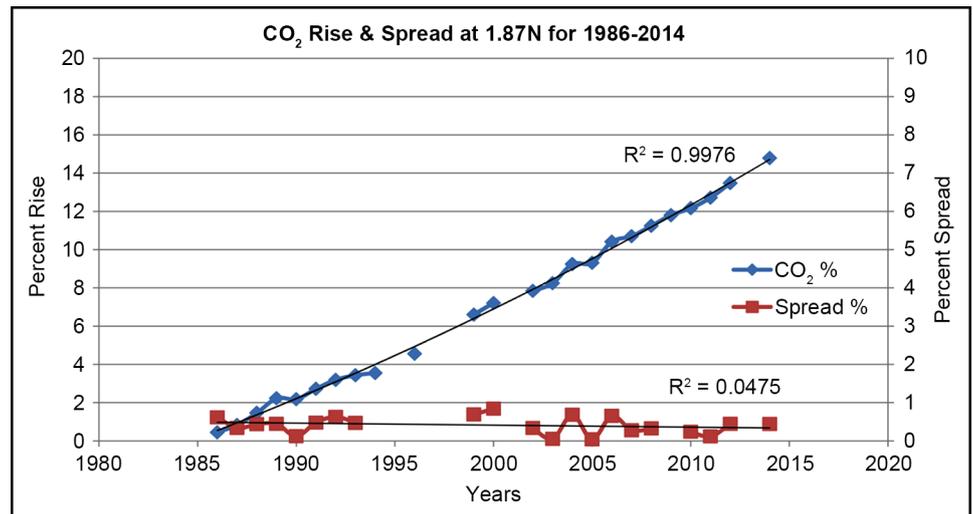
Figure 16. A graph of the percent rise & spread in actual CO_2 near the equator at Christmas Island (1.87˚N).

These dates were selected because many of the sites did not have sufficient data for earlier years. Percent's were used to show relative changes. **Figure 11** is the same plot for Alert, Canada (82.4˚N). **Figure 12** is for Cape Grim, Australia (−41˚S) and **Figure 13** is for Azores, Portugal (38.5˚N). **Figure 14** is for Samoa (−14.3˚S) and **Figure 15** is for Mauna Loa, Hawaii (19.5˚N). These latitudes were selected to compare behaviors occurring at opposing locations in the two Hemispheres. Finally, **Figure 16** is representative of the equator at Christmas Island, Kiribati (1.87˚N).

These figures illustrate that the relative changes in the Northern Hemisphere were very similar to the relative changes in the Southern Hemisphere. For example, the 28 year rise in CO_2 in the Southern Hemisphere changed from 343 ppmv to 393 (Δ50) while the NH changed from 349 ppmv to 401 (Δ52). All of these figures show that the rise was exceptionally smooth exhibiting an R squared statistical variation at 99+ percent while the spread was highly variable with an R squared varying from near zero to a high of 30%. Percentages were used to show relative changes and the side by side comparisons at equivalent latitudes in opposite hemispheres. This provided a means for measuring relative effects from one hemisphere to the other.

The results are shown in **Table 2** in terms of relative change (percent). The Table indicates that the Northern Hemisphere performed in a similar manner to the Southern Hemisphere over a 28 year period. The 28 year period was selected for this analysis because not all of the stations had data going back earlier or there were large gaps in the data.

3.2.3. R Squared & Correlation

R squared is a number that indicates the proportion of variance in dependent variables along the same curve. A high R squared indicates that there is a strong relationship. For example an R square of 1 is a perfect match, meaning that all data points fall on the curve line. There are some caveats that must be considered. R squared does not mean

Table 2. Changes in Rise between Northern Hemisphere and Southern Hemisphere in terms of percent change between 1986 and 2014.

SH Location	Percent Change	NH Location	Percent Change
N Pole (−90˚S)	15%	Alert, Canada (82˚N)	15%
Cape Grim (−41˚S)	15%	Azores, Port (38.7˚N)	15.5%
Samoa (−14˚S)	15.8%	Mauna Loa (19.5˚N)	15.5%
Average SH	**15.3%**	Average NH	**15.3%**

that the independent variables are the cause of the changes in the dependent variables. It may also have a potential bias problem if there are applicable variables omitted. A high or low R squared does not prove/disprove causation in fact. On the other hand, the R squared value is a factor that can be considered in proving causation. It is generally easier to use R squared as a means for disproving a relationship.

Correlation is similar to R squared but deals with different curves. Correlation measures the variance between two curves. It is the average of the summation of each percent deviation between curves at each data point. R squared is how data points fall on a curve and correlation is how two curves match up with each other. A correlation of 100% means that the two curves fall on top of each other. Correlation does not prove causation in fact, but is relevant in proving causation. A poor correlation is strong evidence disproving causation

3.2.4. Variability

Variability and lack of variability are meaningful even in the absence of other factors. High variability suggests that it is probably responsive to large changes. For example, adding 50% of the total to a mixture will show a significant change, whereas adding 0.1 percent may not. Therefore the magnitude of change (Magnitude Factor) will have an effect on the variability. This can be illustrated by the spread (seasonal change) of 4 ppm in the SH and 20 ppm in the NH. This represents about 1 percent (4/400 ppm) change in the South and 5 (20/400) percent change in the North in one year. The yearly rise, on the other hand, is less than 0.5% in both hemispheres. The rise is 2 to 10 times less than spread and reasonably suggests that the larger magnitude would trigger a greater response—and the observational data showed that it did.

Another factor is time (Time Factor). Included in this time factor is the speed in which the product is released, the time it takes a product to mix, and the product's life expectancy. Each affects variability. These time factors may affect the short term and long term variability differently. For example, a product that quickly dies out may have large effects on short term variability but little effect on the long term variability. These time factors may also work in different directions (subtractive) and/or in the same directions (additive).

Release speed, mixing time and product life are independent time variables and are difficult to continuously measure and estimate. Residence time is a combined mea-

surement of product life and mixing time, particularly in the absorption and de-absorption situations. Release time is more independent and more unrelated to residence time. Residence time is an estimate/computation of how long the product stays (in this case) in the atmosphere. The higher the residence time the longer the product will accumulate and the less variable it will become. Carbon dioxide moves into several atmospheric levels (troposphere, stratosphere, and mesosphere) so the volume that must be affected is extremely large. Water vapor on the other hand is mostly limited to the troposphere. This means that the travel distance for CO_2 is larger than water vapor. It may mean that time smooths changes inCO_2 far more than water vapor. Carbon dioxide has a long residence time (most studies put it in the 50 - 100 years) while water vapor has short residence times, *i.e.* weeks to a few months.

The lack of aberrations in the rise data suggests that it has been smoothed by immense volumes (Magnitude Factor) and/or spread over vast distances with a long lifespan (Time Factor). Small fluctuations from sudden environmental phenomena do not appear, *i.e.* volcanoes, winds, hurricanes, monsoons, ocean currents, etc. The "release time" does not appear to be a consideration because the seasonal concentration fluctuations line up with the months and were not shifted significantly. This suggests that the release time is very short—days to a couple of weeks. The changes in volumes (Magnitude Factor) are generally identified in Table 1 and Figures 10-16. The residence time for CO_2 (Time Factor) is addressed hereinafter.

3.2.5. Residence Time

One study [19] set the residence time of carbon dioxide in the atmosphere at 130 years and discussed various published studies on the subject, *i.e.* the IPCC placed it at 5 to 200 years [1], 30 - 95 years [20], and 55 years [21]. Another study placed it at 5 years [22]. Because the CO_2 rise data are uniform and smooth the lower 5 year time period seems unlikely. One study (unpublished) by Roger Andrews in 2014 set forth some convincing evidence that it is 33 years using the Mauna Loa Carbon Dioxide data [23].

The 33 year residence time has been selected for investigation using the Andrews model. With this model, an operative percent for each year is calculated based on the integration or summation of the carbon dioxide concentrations over the last 33 years. In this model the current year has the highest effective percentage (6.4%) and diminishing in accordance with a second order polynomial equation to a zero influence on the 33rd year.

3.2.6. Troposphere Effect

All of the figures and Tables in this article deal with CO_2 concentrations. Concentration is a ratio of the volume of CO_2 to the volume of the air. Most scientific studies focused on the top half, *i.e.* volume of CO_2[3] and do not discuss the bottom half, *i.e.* volume of the air, or they base their analysis on a cubic meter of volume. For a cubic meter of

---

[3]Volume is directly related to mass by converting the mass into moles, *i.e.* dividing the tonnage by the molecular weight of CO_2. GtC divides the CO_2 into the carbon equivalent *i.e.* the ratio of the molecule weight of Carbon (12) divided by the molecular weight of carbon dioxide (44). Mole ratios are identical to the volume ratios.

volume, 1ppmv is the same at the equator as it is at the Poles for the same pressure and temperature. However, when considering the total amount of CO_2 in each Troposphere zone, the volume of the each zone is a component. The earth's circumference and therefore the Troposphere volume varies dramatically depending upon the latitude. In order to compare the effect of releasing tonnes of additional CO_2 into the atmosphere at a particular location there must be a consideration of the volume of the atmosphere at that location. Because of the earth's spin, there are also changes in the troposphere height (7 km at the Poles and 20 km at the equator). As an illustration, the Troposphere volume of the Arctic Circle (90˚N - 66.5˚N) is about ~9.7 times less than the volume of the Troposphere at the equatorial region for the same latitude range (0˚N to 23.4˚N—Tropic of Cancer). Many scientific studies, particularly relating to fossil fuel emissions, appear to equate GtC with ppmv of CO_2 [1] without considering the volume component. This can create a source of confusion. For example, a 1 GtC release of CO_2 at the equator would change the average CO_2 concentration at that location to a value about 9.7 times less than the release of 1 GtC at the Arctic Circle. These volumes are based on a same pressure-temperature ratio between the areas being compared.

The Troposphere effect is substantial, but only in the short term, *i.e.* less than 1year. When CO_2 is released at a particular location, it has an immediate effect at that location. However, over time it is mixed by winds, etc. and the effect diminishes. The vertical mixing in the Troposphere takes about 1 month (less at the polar areas) and the time it takes to mix around the earth is about 1 year. Mixing times can be extremely hard to mathematically simulate because of the differences in winds, pressures, temperatures, and absorptions. Globally, the mixing time is estimated to be about 1 year with the SH being faster and the NH being slower. As such, the Troposphere effect will be less and less significant with the passage of time. It would have large effects on "spread" or seasonal (monthly) fluctuations, but very small effects on rise over multiple years. It would also have an effect on short term "swing" (within a year), but less if it relates to changes over multiple years. It is recognized that CO_2 travels to the stratosphere and mesosphere, however the mixing time in these higher spheres is more than 1 year and were not considered when applying the short term Troposphere effect.

3.3. Causes for the CO_2 Rise

3.3.1. Sea Temperature Rise

Studies have reported connections between rising ocean temperatures and rising CO_2 concentration [2]. The IPCC [1] reported that the total amount of carbon on earth resides in the oceans, which is 6 times more than in the atmosphere. The yearly CO_2 transfer between the ocean and the atmosphere was 182 GtC (90 GtC from the ocean to atmosphere, and 92 GtC in the other direction). Hence the ocean is the largest and most viable candidate for any change in CO_2.

Figure 17 is a graph of the CO_2 increase from 1976 to 2014 at Mauna Loa, Hawaii and the global ocean temperature anomaly. This figure illustrates that the CO_2 rise followed an extremely well fitted 2nd power polynomial curve with the R squared at
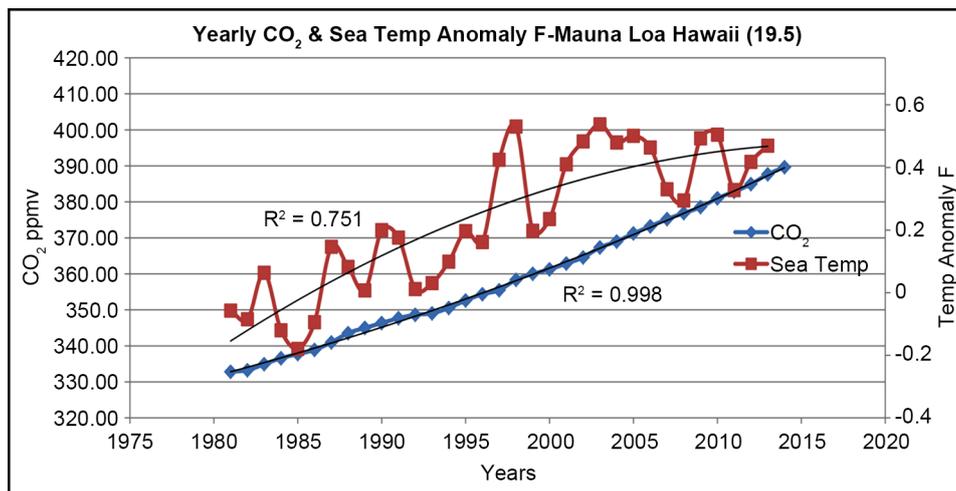
Figure 17. A plot of the CO_2 rise from 1981 to 2014 at Mauna Loa, Hawaii and the world yearly temperature anomaly in degrees Fahrenheit.

99.88%. The global sea surface temperature, on the other hand, was more variable with an R squared of 75% using the same 2nd power polynomial curve. This figure illustrates that both curves appeared to be related as far as the long term upward slope but inversely related as to curvature at the center. As discussed earlier, the CO_2 rise data closely fits a 33 year residence time.

The near surface sea temperature releases CO_2 in various amounts at various locations. This CO_2 does not enter the atmosphere unimpeded nor is there instantaneous mixing. The CO_2 released at the ocean surface in any particular year undergoes many absorption/ejection cycles, biological actions, scrubbing by rains, etc. as it enters the mixing phase in the atmosphere. It should be subjected to the same time smoothing (33 years) as the CO_2.

Figure 18 plots the same data as in Figure 17 except a 33 year residence time (polynomial decay) was applied to the sea temperature. This required temperature data going back to 1949 is available from the EPA and NOAA. Figure 18 shows a good curve match between the two with a correlation of 99.5 percent. It shows that the R square fit went from 75% in Figure 17 to 99% in Figure 18. The curve match correlation does not prove causation. But, like R squared, is relevant in determining causation.

1) Mass Flow Analysis

A mass flow analysis by itself cannot prove causation, but can often be used to disprove it. That is, even if the mass flow calculations show that the temperature increase can cause the observed rise, it does not prove that it did.

There are varying causation hierarchies. If the calculation shows that the product cannot be produced by the occurrence/process, then there is no causation. If the mass flow calculations show that an occurrence/process produces more than the amount needed, then it "can" cause the effect. If the calculations prove that occurrence/process "can" produce a significant portion, but not all, then it may be considered to have a partial causal connection.
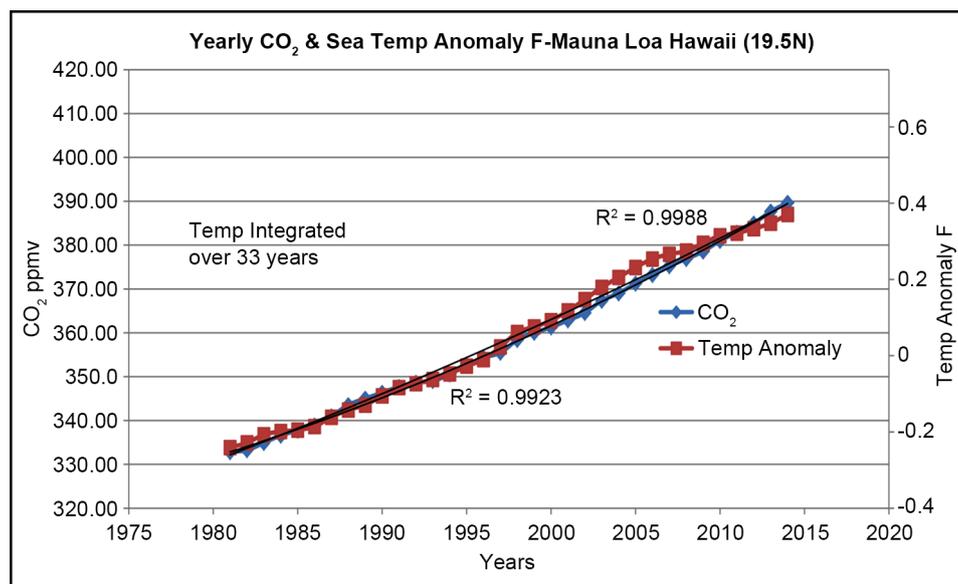
Figure 18. A plot of the CO_2 rise from 1981 to 2014 at Mauna Loa, Hawaii and the world yearly temperature anomaly in degrees Fahrenheit as shown in **Figure 17** except that a 33 year residence time was applied.

2) Mass Flow Calculations

This calculation is directed to whether a 0.7˚ Fahrenheit increase in ocean temperature can cause enough CO_2 to be released to increase the atmospheric concentration by ~60 ppmv over a 33 year period (1981-2014). According to IPCC each 1 ppmv of atmospheric CO_2 equates to 2.21 GtC [1]. The 60 ppmv would therefore require a net 128 GtC of CO_2 to be released from the ocean and spread evenly over the troposphere. The following additional assumptions are made: a) the average amount of carbon in one cubic meter of sea water is 52 grams [24], b) an increase of 1˚F will release 1.5% of the CO_2 dissolved in the water [25], c) the surface area of the oceans is 3.61×10^{14} square meters [26], and d) the top 1 km of the ocean is well mixed over the 33 year period [25]. With these assumptions and information, the net amount of CO_2 released into the atmosphere by a 0.7˚F rise would be ~200 GtC over 33 years which is 64% more than is needed.

The fact that there was 64% more than needed indicates that a portion of the CO_2 released must have been absorbed. The question as to how much is not easily computed. If the atmosphere is considered as a whole, then all of the up CO_2 flux was 197 GtC/yr [1]. The amount being absorbed by plants and the ocean, *i.e.* down flux, was 194 GtC/yr [1]. This shows that almost all of the CO_2 that traveled into the atmosphere was absorbed, *i.e.* 194/197 or 98.48%. There is no reason why CO_2 released from the ocean should be treated any differently than all other CO_2 sources. If this 98.48% absorption factor were applied to the 0.7˚F sea temperature rise, then it would indicate that out of the 200 GtC added by the ocean temperature rise, 196.96 GtC were absorbed yielding a net accumulation 3.04 GtC. The net amount released by the ocean is therefore only 2.3% of the amount needed (128 GtC). The problem about using the IPCC's gross mass

fluxes to calculate absorption percentages is that it is not based on actual absorption data.

Either, the assumptions were incorrect, more than the top 1000 meters of ocean water were involved, the absorption percentage was less than 98.48%, or there were other sources adding to the atmospheric carbon. The obvious answer is all of the above, but "other sources" is the most probable. Other sources include fossil fuel emissions, CO_2 released by fresh water lakes and rivers, changes in land and marine biomasses, soil desiccation, volcanic emissions, chemical processes, etc. There may also be a fundamental error in way the carbon flux was estimated, *i.e.* it is possible that the massive fluxes were back-calculated from an accurate knowledge of the CO_2 accumulation, and not from any precise measurements of actual ocean/biomass breathing. Attempts to estimate this exceedingly complex process would not be verifiable. There may also a potential problem associated with comparing actual CO_2 concentrations with a temperature "anomaly".

Before analyzing the "other sources", there are some unrelated observations from Figure 18. The sea temperature anomaly has some slight deviations, *i.e.* it oscillates under and above the CO_2 every 10 - 11 years. This may be from the influence of a solar signal. It could indicate that the surface ocean temperature should be integrated over a longer time period, such as 50 to 100 years. The figure suggests that the CO_2 is increasing slightly faster than the ocean temperature. Between 1981 and 2014 the increase of CO_2 above the water temperature rise was about 3 ppmv. This equates to about 1 ppmv/decade.

The slight temperature rise of 0.7˚F over 33 years is overwhelmed by the seasonal ocean temperature fluctuations. For example the ocean temperature changed 10˚F at Cape Grim (Figure 22 in Centigrade). That is 14 times higher. This begs the question of how does this effect rise? Several reasons may apply. The strongest is that the seasonal fluctuations are CO_2 neutral, *i.e.*, the increases are offset by the same seasonal loses. There are many push-pull forces that are in play as shown in the vector analysis in Figure 6.

In summary, the exceptionally close curve match indicates that the ocean temperature rise matches the CO_2 rise. The mass flow calculations support the rise, but an absorption factor would need to be applied. After a 98.45% absorption factor is applied, the ocean temperature effect on CO_2 rise is very small, *i.e.* 2.3% of the total.

3.3.2. Fossil Fuel Combustion

The topic of CO_2 associated with fossil fuel burning has been the subject of most Climate Change publications. CO_2 emissions from fossil fuel burning have been increasing since the 1950's. Figure 19 is a plot of the global CO_2 emissions from 1971 to 2013. It is an identical type of graph to Figure 17 except fossil fuel emission (including cement production & gas flaring) tonnage was used instead of ocean temperature. Figure 19 shows that the polynomial curve for the emission data was the best fit with an R squared of 97%. The unintegrated curve shows a steep increase each year.

Figure 20 is the same as Figure 19 except integrated with a 33-year polynomial decay. The emissions curve when compared to the CO_2 curve implies that the CO_2 emitted
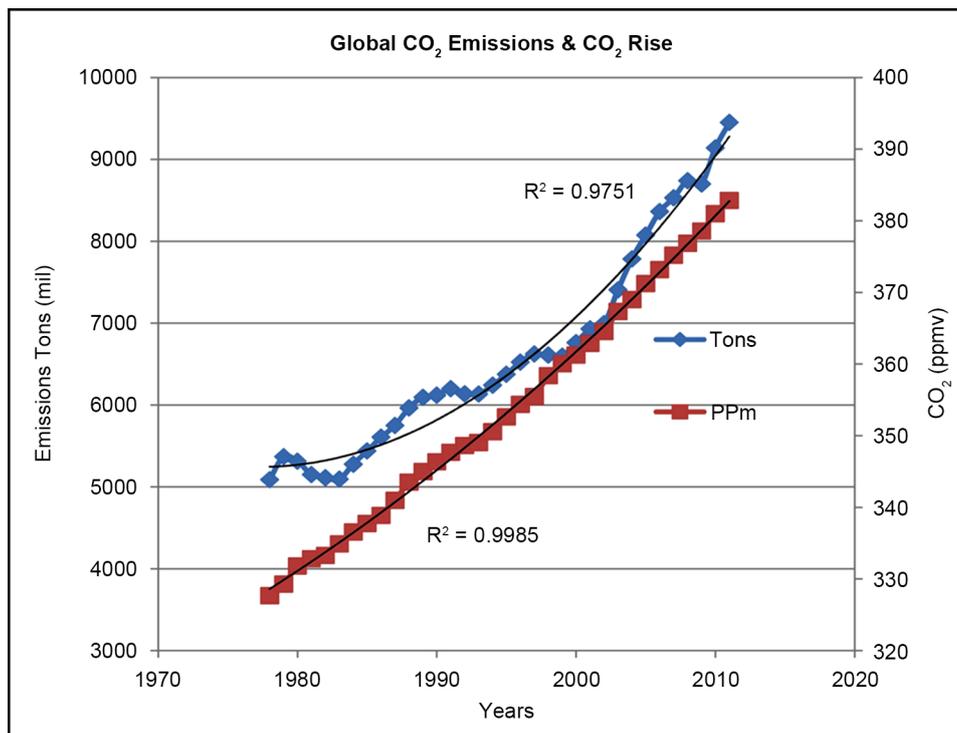
Figure 19. A plot of the world CO_2 emissions from 1979 to 2011. This data is from Tom Boden & Bob Andres of the Carbon Dioxide Information Analysis Center of the Oak Ridge National Laboratory and Gregg Maryland from Appalachian State University.
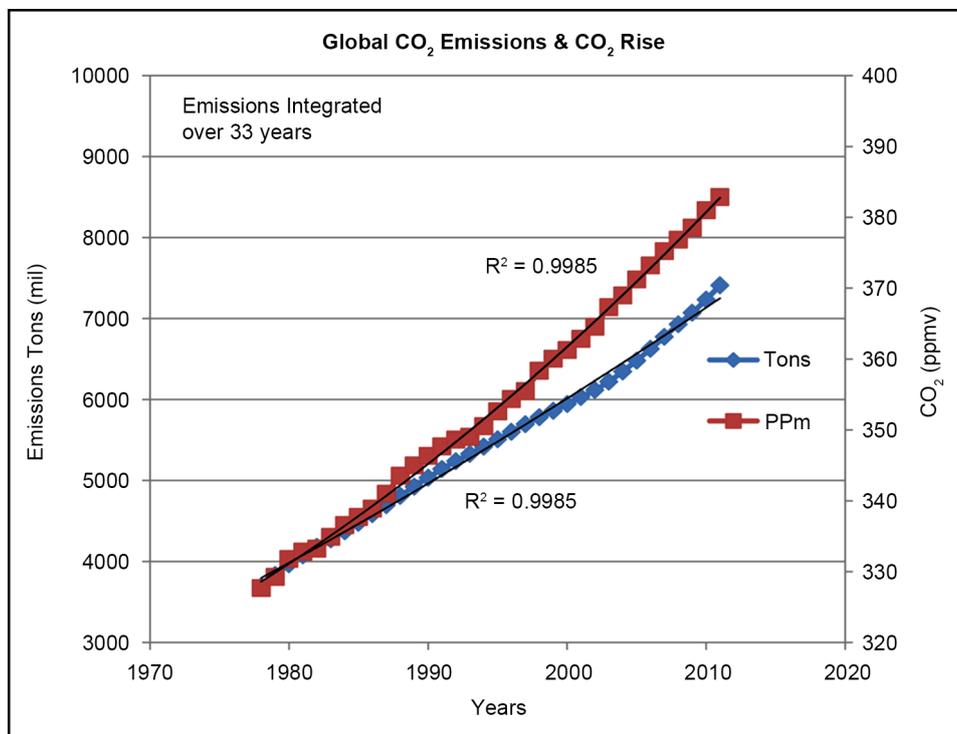

Figure 20. A plot of the same data shown in **Figure 20** except a 33-year residence time was applied to the emissions data.

from the fossil fuel combustion goes directly into the atmosphere unimpeded and mixes within a year. That is not the case. There are many absorption/ejection cycles, biological actions, scrubbing by rains, etc. as the CO_2 enters the mixing phase in the atmosphere. With respect to long term rise, the CO_2 emissions curve should be integrated over the same 33 year period as the global CO_2 rise. Both curves show an R squared value above 99% indicating that the data supporting each curve is exceptionally consistent.

Figure 20 shows that the two curves do not match up. The correlation between the curves is good between 1979 and 1985, but after 1985 it falls off. The CO_2 rise is increasing faster than the CO_2 emissions, which suggests that the emissions were not the cause for the rise. The curve data in Figure 20 suggests that the fossil fuel emissions contribute to the CO_2 rise but at a different slope. Having a different slope does not negate fossil fuels as a major cause of the rise because other causes could fill in the gap.

An engineering mass/volume analysis can be performed based on the IPCC's statement of 5 GtC/yr. This amounts to 165 GtC over 33 years. The amount needed was 128 GtC. Hence there was 37 GtC more than required, *i.e.* 29% too much. Applying a 98.48% absorption factor to the emission release provides a net of 1.94 GtC or only 1.5% of the total amount needed.

Proof that Absorption Percent is High. There are seasonal observations that support a large absorption percent. The CO_2 concentrations at the stations located above, below and to the west of the United States were plotted on one Y axis and US CO_2 emissions tonnage was plotted on the other Y axis. A comparison between the three stations showed no influence by or from the emissions. This is discussed more fully in section E subsection c hereinafter and graphically shown in Figure 23. Similar comparisons were made for other years with no observed connection. These observations support a high absorption rate.

The Troposphere effect, as discussed hereinbefore, supports a large absorption percent. According to the IPCC the fossil fuel emissions were 5 GtC/yr [1]. Ninety percent of these emissions occur in the NH between the latitudes of 30°N to 60°N, which means that 4.5 GtC would be released in that segment of the Troposphere. Figure 21 is a plot of the GtC emissions on the Y axis and the Troposphere volume on the X axis divided into eighteen 5-degree latitude zones stretching from the equator to the North Pole. Each line represents the average concentration of CO_2 in the Troposphere zone expressed in parts per million (ppm)[4]. The blue box is the zone between 30°N and 60°N where the CO_2 emissions are released. This figure shows how much carbon (GtC) is in each zone to yield an average ppmv concentration in the Northern Hemisphere. For example the amount of carbon in the 5 degree zone ending at the north pole is extremely small (0.00086 GtC) for a 1ppmv NH average whereas the amount at the 5 degree zone at the equator is much higher (0.112 GtC). Figure 22 is the same as Figure 21, except that there is an assumption that 90% of the fossil fuel emissions are released

---

[4]For line "1ppm" if all of the GtC for each 5 degree zone are added together, they would equal 1.07 GtC, *i.e.* the amount of CO_2 in the entire Troposphere (2.14 GtC) divided by 2 because the graph only relates to one hemisphere.
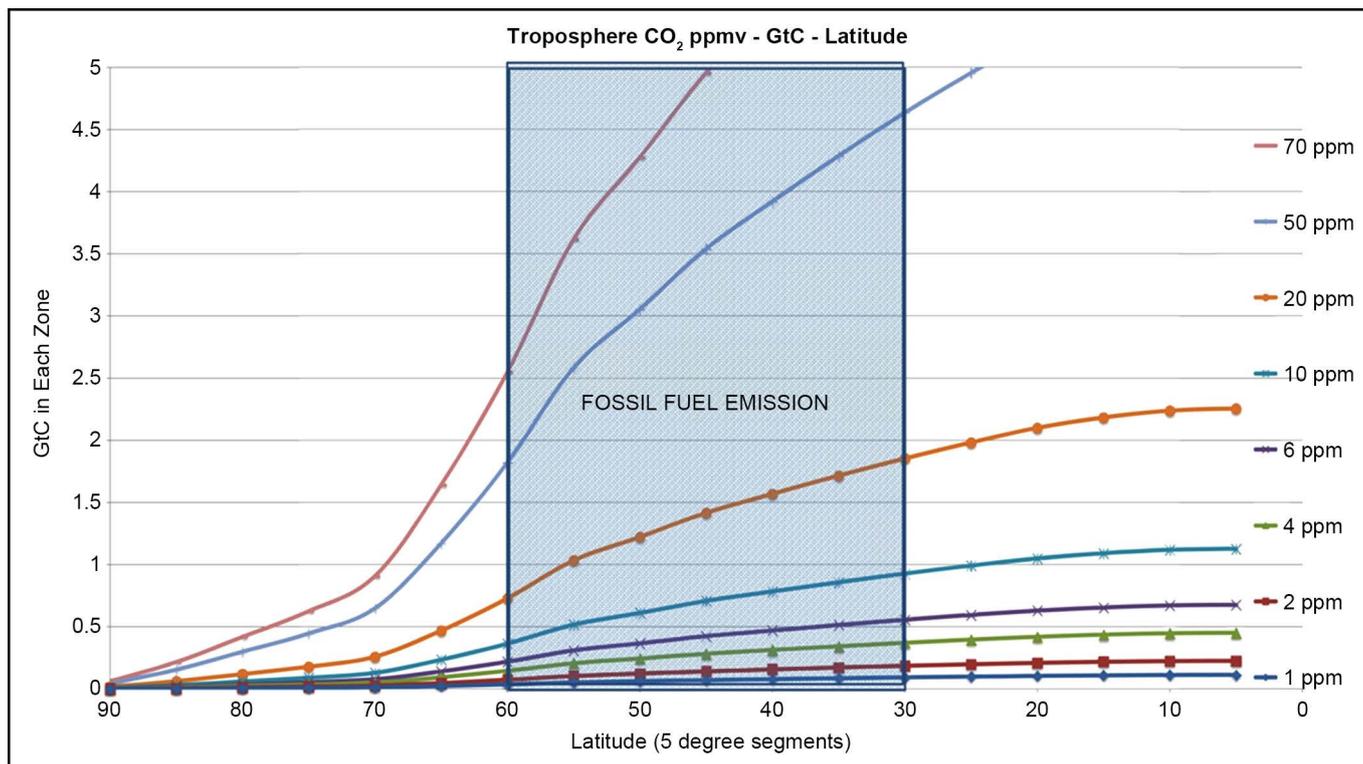
Figure 21. Plot of Troposphere in the Northern Hemisphere in 5 degree increments along the X axis. The vertical axis is the amount of CO_2 in GtC for each line referencing a different average CO_2 concentration expressed in ppmv.
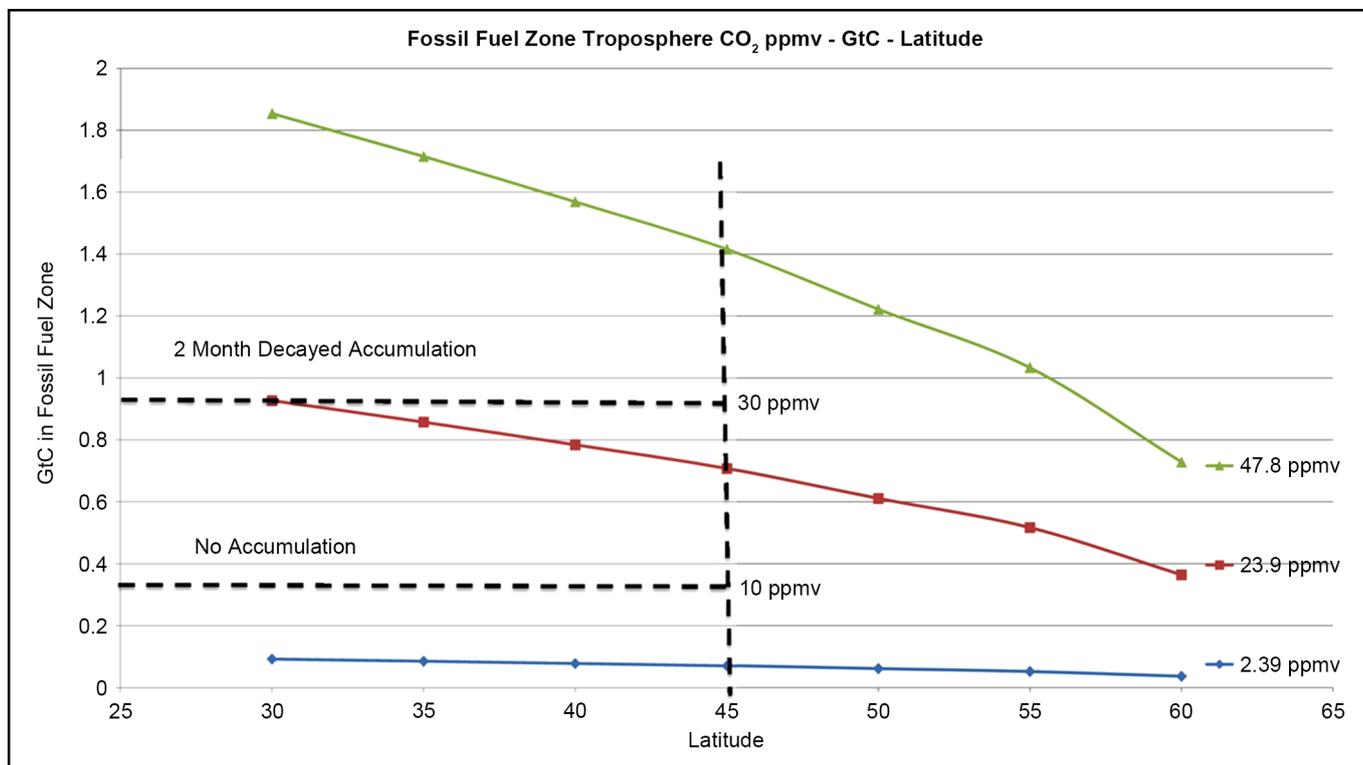

Figure 22. Same as **Figure 21** except limited to the Fossil Fuel Zone 30˚N to 60˚N.

only in the zone between 30˚N to 60˚N. The fossil fuel emissions (4.5 GtC) are not released in one moth, but over 12 months at approximately 0.375 GtC/month. This is shown by the bottom dotted line. This line assumes that there is no accumulation between months from the release. The vertical dotted line is the middle of the fossil fuel zone. Where it intersects the bottom dotted line is at concentration of 10 ppmv. That is, the average concentration in the fossil fuel zone would go up by 10 ppmv because of the release of 0.375 GtC in one month. The actual observations from stations at those latitudes and compared to others stations showed no measurable effect from the emissions. Hence, a very large absorption must be occurring. In addition, a one month mixing period in that zone is too fast. The second dotted line is a 3-month mixing period where a portion of the CO_2 released in the two prior months are added. But it is seriously decayed by a polynomial reduction, *i.e.* 50% of the previous month and 10% of the month before that are added. This is more realistic and shows that the release of CO_2 would increase the concentration in the fossil fuel zone by approximately 30 ppmv. This supports a very high absorption percentage.

In summary: 1) the graphic correlation set forth in **Figure 20** indicates that the CO_2 rise and emissions curves did not match; 2) the mass flow calculations showed that fossil fuels could produce more CO_2 than was necessary, but more information is needed as to the actual absorption percentages; 3) the total amount of CO_2 released in the air and the total amount absorbed each year supports a 98.48% absorption rate, 4) the actual short term observations set forth in **Figure 25**, infra, supports a high absorption rate, 5) the Troposphere effect shown in **Figure 22** supports a high absorption rate, and 6) the hemispheric balance shown in **Table 2** supports a high absorption rate. Considering all of these factors, it is more likely than not that fossil fuel emissions have a very small effect on the rise in CO_2, *i.e.* 1.5%.

3.3.3. Other Causes.

There are many other causes that contribute to the CO_2 rise. A few of these include the following:

1) Animal Biology

Biology is the second biggest contributor of CO_2 emissions/absorption after the ocean. Biology is also the most difficult to predict. Plants play the major role in consuming CO_2 (sinks) but non-plant biomass plays the major role in releasing CO_2 (sources) both by respiration and by detritus (decay). Surprisingly, the largest by weight in the non-plant kingdom are the small. Bacterial biomass may constitute as much as 350 - 550 billion tonnes and equals 60% to 100% of all the carbon in all the plants [27]. The insect group is next. For example, the weight of just two insect species (ants and termites) is 745 million tonnes, which is 2.1 times greater than the weight of all humans [27]. And there are 1 million insect species.

Both bacterial and insect density are temperature related. An increase in global temperature over the last 33 years translates into an increase in bacterial and insect density. Hence, this is a viable candidate for the majority of the CO_2 rise. Unfortunately biology is massive, complex, and impossible to catalog accurately. Therefore, a mass calculation

cannot be performed accurately.

2) Land Soil

The land soil contains 2 - 4 times more carbon than the atmosphere [28]. The IPCC shows that the amount being absorbed by the soil and detritus was 50 GtC per year and that 50 GtC/yr of CO_2 were returned [1]. That is 100 GtC exchanged per year. If this is off by 1 percent it would account for 33 GtC over 33 years.

3) Volcanic/Tectonic Events

The IPCC believed that CO_2 emissions from volcanoes or tectonic events were too small to be considered and did not show that source on their carbon cycle analysis [1]. However, it has now been discovered that the previous CO_2 estimates were seriously underestimated [29]. New estimates place the yearly CO_2 emissions slightly less than 1 GtC/yr. (33 GtC over 33 years). After the Burton study was published, researchers discovered a 1500 meter long range consisting of hundreds of active submarine volcanoes off the coast of Norway [30]. Hence, the ~1 GtC/yr CO_2 ejections may be underestimated.

4) Chemical Processes

The ejection of acidic gases from volcanoes and production of commercial acids have resulted in these acids accumulating in the air, soil and oceans. The acids enter the water cycle and decrease the ocean pH. These acids react with carbonates (marble, limestone, marine animal shells, etc.) and produce CO_2. The size of this chemical process is not known, but with SO_2 being one of the dominate gases emitted by volcanoes, it will produce at least as much SO_2 as CO_2. The global commercial sulfuric acid production is estimated at 230 million tons/year. Although most of these acids are neutralized prior to entering the water cycle, it is likely that a significant amount finds its way into the ocean. In addition some of the sulfur from the neutralized acid is eventually re-oxidized to form SO_2 which in turn is converted to sulfuric acid in the atmosphere.

In sum, the "other sources" are viable and could account for the 128 GtC required to increase the concentration by 60 ppmv over the last 33 years.

3.4. Causes for the Swing

The causes for changes in the CO_2 concentration between latitudes, *i.e.* swing, have been investigated, but a satisfactory explanation has not been established. The changes in swing in the NH, as shown in Figure 9, appeared similar to the increases/decreases in the specific humidity over the same years. However, the observed data do not support a direct humidity connection. The fossil fuel emissions curve shown in Figure 19 does not exhibit the same slope or shape as the swing curve shown in Figure 9. The swing change in the NH increased by ~17.5%, whereas the emissions increase during that period was 90% (Figure 19) and 100% (Figure 20). This does not support direct connection with fossil fuel emissions.

There appeared to be a connection between "rise" and "swing" in the NH. That is, the percent rise and the percent increase in spread with latitude over many years appeared similar. An increase in spread as it applies to latitude translates into an increase

in swing. One mechanism considered was that the slow accumulation of CO_2 each year (rise) causes a temporary increase in the amount of CO_2 absorbed by snow melt. When the snow melt evaporates, it releases slightly more CO_2 into the air. However, the swing change (increase) in the NH was ~17.5% between 1986-2014 while the rise in the NH was 15.3% (Table 2). Contrast that with a near zero swing change during that period in the SH but having the same rise, *i.e.* ~15.3%. This negates a link between the two. It is possible that the southern ocean sink has a small effect on swing but not on rise, and/or that land has a larger effect on swing than rise. It is also possible that long term rise cannot be compared to swing because former has a 33 year residence time as modulated by the stratosphere and the other does not.

The major differences between the NH and the SH is that the north is land-locked whereas the ocean swirls around Antarctica. The land biomass in the north exceeds the land biomass in the south, but the marine biomass is greater in the south. Fossil fuel emissions are 90% higher in the north. The temperature fluctuations are higher in the north and cooler in the south. Significant snowfall change exists outside the Arctic Circle but not outside the Antarctic Circle. This study could not find a strong connection of these factors as it relates to swing.

In sum, the causes for changes in the swing remain elusive.

3.5. Causes for the Spread or Seasonal Fluctuations

This section addresses causation of the monthly fluctuations.

3.5.1. Bio-Respiration

Biology is one of the most powerful and misunderstood forces controlling environmental conditions on this planet. The plants and animals are only a part of what biology has created. All of the oxygen in the atmosphere is attributed to biological actions. Most of the iron oxide we mine is the result of biology. Marble, limestone, and many other minerals would not exist but for biology. Because of this power, consideration of biology must be included in any analysis. Unfortunately, biology has creative ways of disregarding attempts to restrain it by mathematical formulas.

Keeling and others have observed that the CO_2 seasonal cycle mirrored the growing season (May-September) when land plant photosynthesis was in full swing and the dormant season (November-April) when land plant respiration was active. Observations showed that photosynthetic drawdown appeared to occur more in North America while respiration dominated in Eurasia. The studies reported a strong inverse relationship between CO_2 concentrations and annually averaged Northern hemisphere land temperatures. The average land & air temperatures could be used as a proxy to predict the biological activity, *i.e.* warmer periods equated to more plant growth and colder periods reflected more respiration. Proxies are valuable in explaining general biological phenomena as well as paleoecology.

One study [3] compared CO_2 seasonal fluctuations to seasonal changes in the Normalized Difference Vegetation Index (NDIV). This index measures the amount of green light reflected from the land plants. It is used to estimate plant growth, health,

and expansion.

It is a ratio in reflectance between visible light and near infrared. This reflectivity can be observed by satellites for a global analysis or by drones for a closer and more accurate measurement. The NDIV parameter is indeed a more accurate and valuable proxy in measuring photosynthesis (not as much on respiration) than land temperatures alone. There are many models that have been proposed for estimating leaf phenology [31].

However, NDIV has some limitations. The instruments cannot measure signals through clouds, and it detects canopy leaf surface area and not volume. The signal is also degraded by changes in soil reflectance, leaf optical properties, leaf orientation, viewing angle, backscattering, forward scattering, changes in humidity, and numerous other factors [32].

Current scientific studies support a biological connection as a predominate cause for the seasonal CO_2 fluctuations. But none of these studies have explained how higher CO_2 concentrations occurring at the Polar Regions can exist where there is very little land biomass. This study **adds** to the biological connection.

3.5.2. Sea Temperature Changes

Twice as much carbon dioxide can dissolve in cold water [25]. When the oceans warm, CO_2 should be released into the atmosphere. Therefore, rising sea temperatures will cause a rising CO_2 concentration and visa versa. This is a direct relationship in accordance with Henry's Law. **Figure 23** is a plot of sea temperatures around Cape Grim and the CO_2 concentration. This plot is representative of the CO_2 fluctuations & sea temperature variations at other locations and latitudes, except near the equator where the two hemispheres are transitioning. However, this figure shows that the relationship is not direct. It is opposite (inverse). A rising temperature causes a declining CO_2 and visa versa. This inverse relationship is readily apparent in **Figure 24** where the sea temperature scale was reversed.

A plausible explanation for this inverse relationship is that the rising/falling sea temperature **does** cause CO_2 to be released/absorbed as Henry's law predicts, but an off-setting phenomena must be occurring simultaneously. In this regard the sea temperature would be acting both as a source/sink and as a proxy.

A proxy is an observation/characteristic that changes in the same way that some other observation/characteristic behaves. For example, the oxygen 18 isotope contained in glacial ice cores is used to infer historical temperatures existing at the time the ice formed. The oxygen18 isotope does not cause temperature changes but it can be used to predict such changes. In this example oxygen 18 acted as a proxy.

Can ocean seasonal temperature variations be acting as a proxy?

1) Proxy—Biological Connection

The land/air temperature and CO_2 relationship is inverse. Scientists used this inverse relationship as a proxy to connect CO_2 from biology with land/air temperatures. This is discussed in section E subsection a. The relationship between sea temperature and phytoplankton activity may have viability, *i.e.* the higher temperatures increase
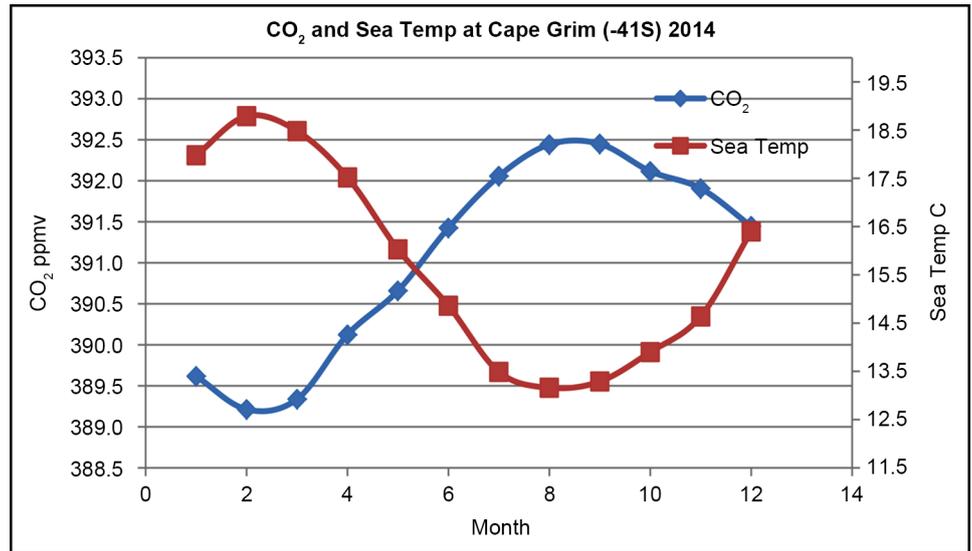
Figure 23. A graph of the CO_2 concentration and average monthly sea temperature in degrees Celsius. The sea temperature data are from the United States Environmental Protection Agency, a division of NOAA.
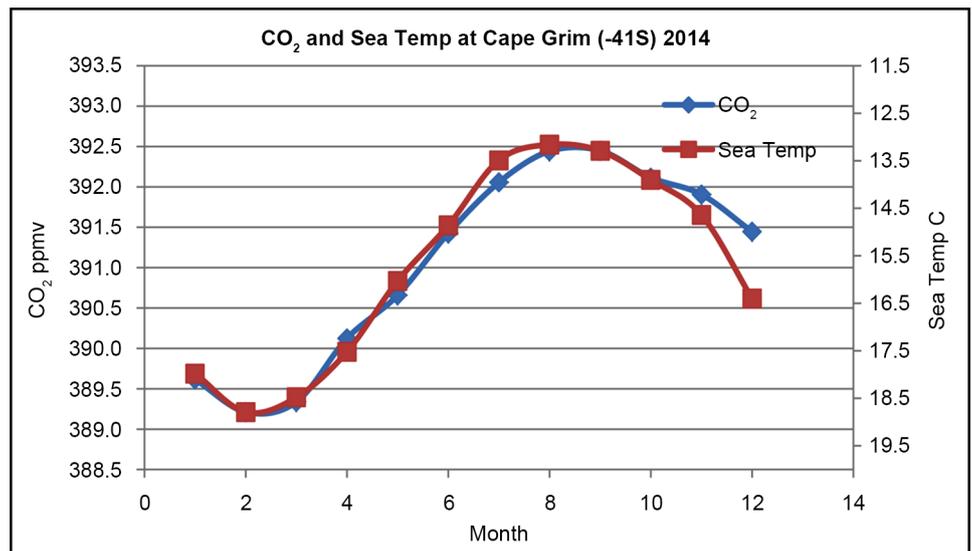

Figure 24. This is the same as **Figure 23** except the sea temperature scale is reversed., *i.e.* descending rather than ascending.

phytoplankton activity which in turn consumes CO_2. Unfortunately, there is insufficient published data available to plot this correlation. This needs to be the subject of further scientific investigation. Until such a study is completed, this potential explanation remains unknown.

2) Proxy—Rain Connection

There is a general relationship between increasing ocean temperatures and increasing ocean rainfall [33]. This would support an inverse relationship. Rainfall is an effective mechanism for scrubbing (removing) CO_2 from the atmosphere. When rain forms it

creates massive numbers of tiny droplets of pure water. These droplets have a surface area thousands and thousands of times greater than the droplets that hit the ocean surface. CO_2 absorption is directly related to surface area of these droplets. Hence, rain, particularly high in the atmosphere, will effectively remove CO_2. If rising ocean temperatures increase rainfall, and rainfall decreases CO_2, then this would support the inverse relationship as observed. The rain/temperature/CO_2 relationship has not been investigated in this study. Until such investigation is completed, this potential explanation remains unknown.

3) Proxy—Ocean Humidity Connection

Humidity (Figure 1) and CO_2 concentration (Figure 5) exhibit an inverse relationship. Plots of humidity on a reversed scale and CO_2 concentration are remarkably in sync. Numerous graphs were made with data from many stations covering multiple years and all showed a good correlation. This is not unexpected since ocean humidity and ocean temperature are directly related. Humidity and rainfall have a closer connection than sea temperature and rainfall. On the other hand, sea temperature and marine biological activity are more closely related than humidity and marine biology. If rainfall governs the relationship, then humidity may be a better proxy. If it is controlled by marine biology, then sea temperatures may be a better proxy. There is a need for more research in this area.

4) Delay Times

Delay or lag times may provide an explanation. If the sea water temperatures and CO_2 concentrations are off by 6 months then the sea temperature and CO_2 concentration curves are in sync. A delay or lag time is a scientifically valid mechanism. If ocean water ejects CO_2 as the solubility laws project, then there would be delay with the CO_2 mixing in the atmosphere. However, connecting this delay to exactly six months seems unlikely. Until a study is completed on this issue, this explanation is unknown— but questionable.

In summary, until there are plausible reasons based on sound engineering principles why atmospheric CO_2 fluctuations and sea temperature fluctuations should have an inverse relationship, it should be considered scientifically viable but uncertain.

3.5.3. Fossil Fuel Emissions

Figure 25 is a plot of US fossil fuel emissions and seasonal CO_2 fluctuations at the Azores, Portugal (38.7˚N) in 2003. The figure shows no apparent relationship between the curves. The emissions curve is contrary to the CO_2 concentration rise & fall in 9 out of the 12 months (Jan and Mar-Oct). The Azores are directly east of the US. The Azores CO_2 monthly curves were very similar to the other CO_2 curves at different stations, including Iceland to the north and Barbados to the south. The US emissions appeared to have no measurable effect on any of the curves.

Comparison of Azores CO_2 data with Midway (same latitude) over several years of relative ratios, anomalies differences, slopes, shapes, and other curve properties showed no detectible correlation with emissions. The same comparisons were done with global emissions with the same results.
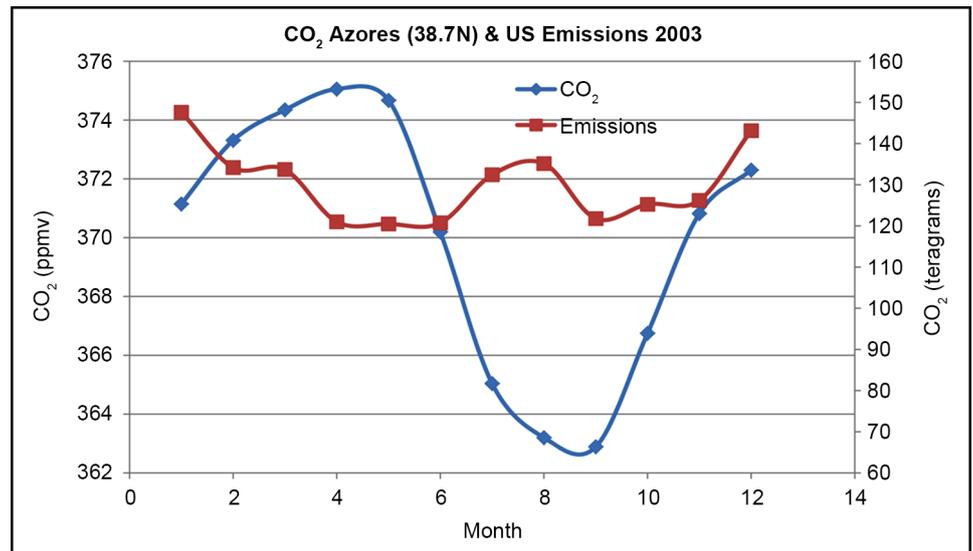
Figure 25. CO_2 Concentration data for Azores in 2003 from NOAA and US CO_2 Emissions data for 2003 from Oak Ridge National Laboratory & Oregon State University.

A comparison was also made based on the assumption that the 1.6 ppmv yearly rise was caused entirely from CO_2 emissions. This also showed no detectible correlation. A relative comparison with stations in the Southern Hemisphere, including Eastern Island ($-27°S$), showed no detectible correlation.

In summary, the lack of a graphical relationship between emissions and CO_2 concentrations, the fact that the Azores curve showed no measurable response to the US emissions when compared over multiple years and multiple stations, and the lack of scientific studies to the contrary, supports the conclusion that there is no likely connection between fossil fuel emissions and seasonal fluctuations.

3.5.4. Sea Ice and Snow Changes

The published studies have not adequately addressed why the highest CO_2 concentrations occur at the highest latitudes, *i.e.* North and South Poles. There is very little biological activity at these latitudes and sea temperatures work in the opposite direction.

On the other hand, there are scientific studies connecting CO_2 ejection during sea ice formation [34]-[36]. This phenomena has been known for years in commercial sea water desalinization processes. The most obvious desalination method is by distillation. However, this same process works by freezing. When sea water freezes, all of the CO_2 that is bound up in that water is forced out. Not only is the dissolved gaseous CO_2 released, but all of the CO_2 held in the carbonate form is released as well. Therefore, sea ice freezing is a viable mechanism for directly producing/ejecting CO_2 (sources). In the spring when sea ice begins to melt (Oct in Antarctica and April in Arctic) it may act in the other direction (sink) [37] [38].

1) Snow Area

Snow is produced in large quantities and spread out over vast areas in the NH. The 2011 change in snow coverage averaged about 25×10^6 square km, but varied from $49 \times$

10^6 to 2×10^6 square km. Significant snow does not exist outside Antarctica due to the Southern Oceans, and as such, snow cover does not change significantly.

There is insufficient evidence that snow produces CO_2 directly. However, there are valid engineering principles, which show that snow does have an indirect effect. When snow covers the ground it inhibits the soil moisture from absorbing/releasing CO_2. Inhibiting absorption has the same effect as producing CO_2 relative to concentration. In addition, when snow thaws the fresh snow melt quickly absorbs CO_2. This snow melt then enters the ground, *i.e.* tundra. Therefore, snow has a significant causal connection the CO_2 seasonal cycle.

2) Mass Balance

This computation is directed to whether ice formation and snow can cause enough CO_2 to be released to effect a change in the atmospheric concentration. The analysis is directed to the NH because that is where the greatest fluctuation occurs. The IPCC [1] reports that 2.14 GtC are contained in each ppmv in the global atmosphere. The following criteria was used in this calculation: 1) the volume in the Troposphere is $\sim 8.4 \times 10^{18}$ cubic meters; 2) the volume of Troposphere in the Arctic Circle is $\sim 1.4 \times 10^{17}$ cubic meters; 3) the sea ice surface area change in 2011 was reported to be 6.07×10^{12} square meters; 4) the average ice depth is 3 meters; 5) the average dissolved CO_2 in sea water is 52 gm of carbon per cubic meter [24]; and 6) the average CO_2 spread is ~ 20 ppmv. Based on this information, then the amount of CO_2 needed in the Arctic Circle for a 20 ppmv rise would be 0.7116 GtC. The amount released by freezing ice would be about 0.93 GtC. This calculation shows that the ice freezing process "can" provide 30% more CO_2 than needed. It is therefore viable.

The fact that it produced more than needed also suggests that there is some of the CO_2 absorbed. However the absorption rate applicable to the world (98.45%) rate should not apply to the Arctic Circle. For example, this area is primarily covered by land or ice throughout the year. That restricts the ocean area available for absorption. There is no significant biomass in this area available for photosynthesis. Since these two sources/sinks are responsible for 98% of the CO_2 flux, these factors will substantially reduce the amount of absorption. What absorption percentage applies is not known, but more likely than not it would be substantially less than 50%.

3) Southern Hemisphere Ice

The SH has about twice the amount of surface sea ice change each year compared to the NH. The amount was approximately 11.88×10^6 square meters in 2011. The change in sea ice was similar for each of the years and is representative. The depth of the sea ice in the SH, however, is thinner (between 1 to 1.5 meters thick) than in the NH, making the ice volume change slightly higher in the NH. The CO_2 spread in the SH is very different. It is 2.5 - 3 ppmv versus 20 in the north. The volume of ice change should have produced a larger CO_2 seasonal spread than observed. One explanation is that the sea ice is immediately adjacent to a large CO_2 sink, *i.e.* the southern ocean, whereas the Arctic Circle is mostly land-locked. The southern ocean is cooler than the northern oceans and this increases it ability to absorb CO_2. The release of CO_2 from the ice is

therefore likely absorbed by the cooler Southern Ocean.

4) Ice Boundary.

The greatest CO_2 fluctuation (spread) is not at the South Pole, but closer to where the ice sheets are formed (see Table 1). The South Pole ($-90°$S) spread is 3.02 ppmv (covered by ice year around), at Palmer Station it is 3.68 ppm(covered by ice half the year) and at Ushuaia, Argentina (54.8°S) is 4.12 ppmv (no ice coverage during the year and protected by land to the north).This suggests that the CO_2 was coming from the boundary where sea ice freezes and not from the South Pole itself. The NH reveals the same effect. Alert (82.4°N) has a spread of 18.3 ppmv (mostly covered year around), Barrows, Alaska (71.4°N) at 20.8 ppmv (covered half the year) and Cold Bay, Alaska (55.2°N) at 20.2 ppmv (covered part of the year but exposed to open ocean). These factors all point to the sea ice and ocean freezing boundary as the major CO_2 source.

5) Sea Ice & Snow Curves.

The final analysis is whether there is a good correlation between seasonal sea ice/snow and CO_2 concentration. The sea ice and snow areas used in this analysis are based on 2011 data. However, as can be seen in Figure 26 and Figure 27 the sea ice and snow changes are relatively small and would have minimal effects in this analysis. The ice and snow data are from the National Snow & Ice Data (NSIDC) 2008 University of Colorado, Boulder, Colorado USA doi http://dx.doi.org/10.7265/N52R3PMC, data set G02156. References to NSIDC are to this data source. The sea ice area cannot be added to the snow area because there is a considerable difference in equivalent water content. The snow cover is therefore reduced by using the water content value, *i.e.* 10% of the snow represents liquid water.

A geographic adjustment is applied because the snow cover extended to 30°N latitude in the NH. At that distance, the snow would have no measurable effect on polar
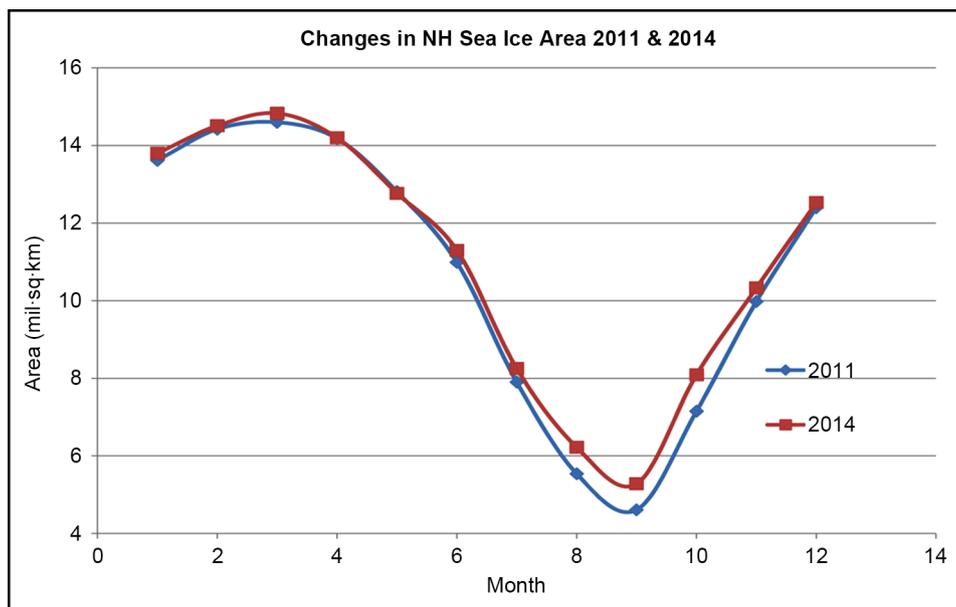

Figure 26. Monthly sea ice area in NH in 2011 and 2014 from NSIDC.

fluctuations. It is also recognized that because of the Troposphere Effect, the snow at the lower latitudes would have a negligible effect. As such, the snow is divided into three groups according to the location.

Figure 28 plots the snow cover area for various latitude brackets, *i.e.* 60 to 90 degrees in group 1, 45 to 60 degrees in group 2, and 35 - 45 degrees in group 3. The grouping and percentage of snow cover were estimated from 2011 satellite images.

The snow in group 1 (60˚N to 90˚N) will have a small effect on the CO_2 in the Arctic Circle. The ice formation would have the most effect. The snow arrives earlier (mid-August) and melts later (May).
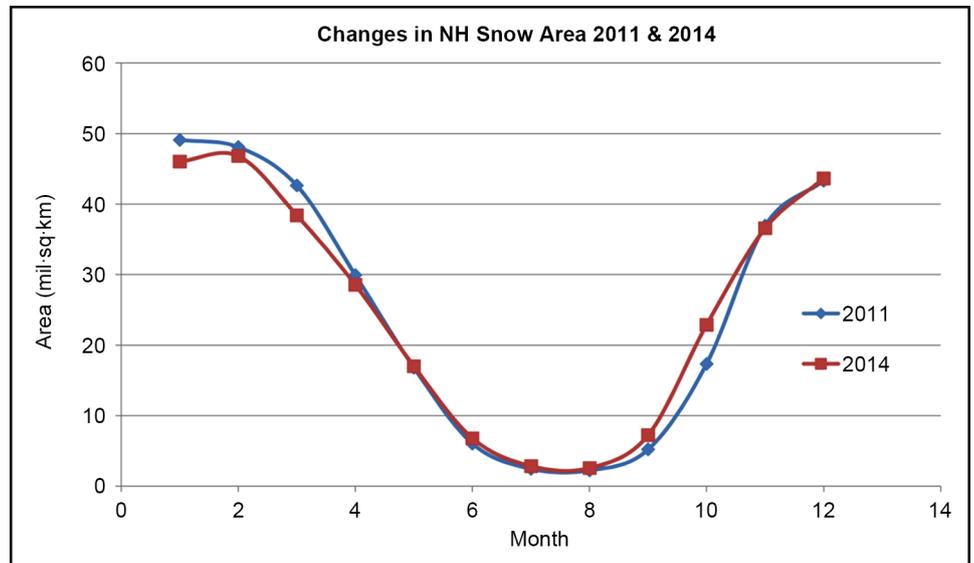

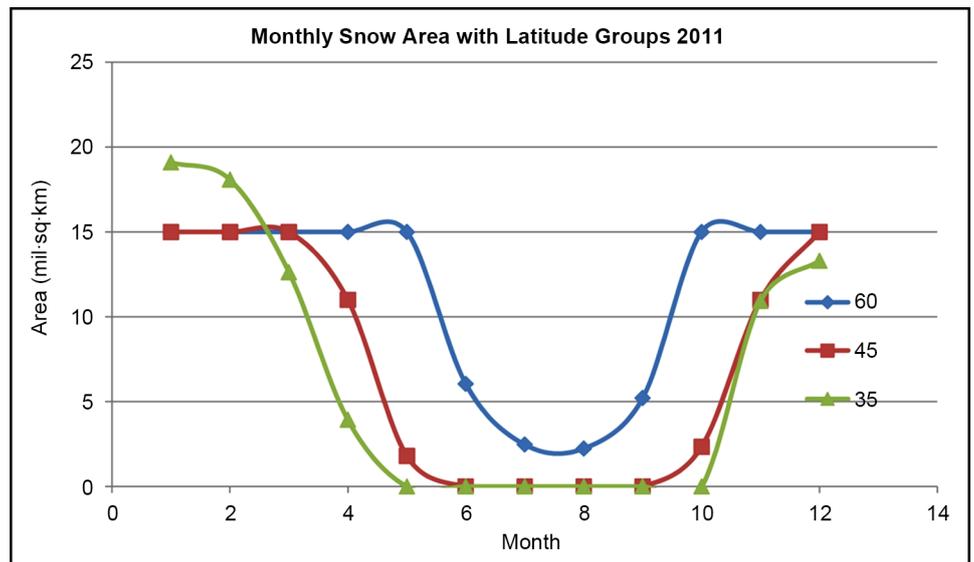**Figure 27.** Monthly snow area in NH in 2011 and 2014. Snow data from NSIDC.

Figure 28. A graph of snow area groups expressed as snow coverage area in 2011. Snow data and satellite photos data from NSIDC.

The snow in group 2 (45˚N - 60˚N) typically arrives in mid-September and continues until March. The melting process begins in March and ends in May. The snow in this group would have very little effect on the CO_2 concentration in the Arctic Circle because of the mass flow vectors shown in Figure 6 and the troposphere volume increase. It may have a small effect on the stations located within the group 2 zone.

Snow group 3 (35˚N - 45˚N) is the furthest away from the Polar Regions. In this group the snowfall began in October and continued until January. The spring melt started in February and lasted until May. The snow in this group would have no effect on the polar regions since the group 3 distance is considerable, the troposphere volume is much higher, and the concentration flux in the northern direction would impede flow in that direction (see vector analysis in Figure 6). Group 3 snow would have little, if any, effect on the CO_2 concentration within this 35 - 45 degree latitude spread. However there may be a significant biomass effect that may be repressed by the snow.

The snow effect in this analysis only considers the freezing/absorption effects. Figure 29 and Figure 30 are graphs in which sea ice & snow areas are plotted on one Y axis and CO_2 concentration is plotted on the opposite Y axis for Barrows, Alaska (71˚N) and Cold Bay, Alaska (55˚N) for 2014.

These figures show a correlation above 90%. A 90% correlation is exceptional and supports a good relationship. Each of the stations in the Northern Hemisphere have a sea ice & snow scale of 0 to 20 million square kilometers. The CO_2 concentration may be different between stations to reflect the differences between latitudes, but the same scale of 30 ppmv was used. For example, the sea ice & snow scale in Figure 29 for Barrows, Alaska illustrates 0 - 20 million kilometers for sea ice & snow and a 30 ppmv scale for the CO_2 concentration, *i.e.* 379.8 to 409.8. The sea ice & snow scale in Figure 30 for Cold Bay, Alaska carries the same scales, *i.e.* 0 - 20 million kilometers for sea ice & snow and a 30 ppmv scale for the CO_2 concentration, *i.e.* 378 to 408.

There were a few discrepancies between the curves, which is reflected by the 90% correlation.

Figure 29 (Barrows) showed that the freezing process (ice + 0.1 snow in group 1 only) began in September 2014 and extended to December (6 million km^2 to 14 million km^2). This constitutes about 87% of the total. The remaining 13 percent of the freezing occurred between December and March. Hence, the vast amount of CO_2 released should have happened during this time. This is consistent with the CO_2 curves. The melting period began in March and ended in September. The figure also shows that the rise in freezing initially led the CO_2 rise (Sep-Oct) and then lagged behind the rise (October- January). During the melting process the ice melt led the CO_2 drop (April-July) and then lagged behind it (July and August). Ice formation should **lead** the CO_2 rise and ice melt should **lead** a drop in CO_2. In other words, freezing needs to release CO_2 before it can accumulate and ice needs to melt before CO_2 can be absorbed by it.

The lag time between the ice release of CO_2 (freezing) and the concentration rise is not known, nor is the lag time known between ice melt absorbing CO_2 and the drop in concentration. The small area in the Arctic Circle would likely make any time lag less
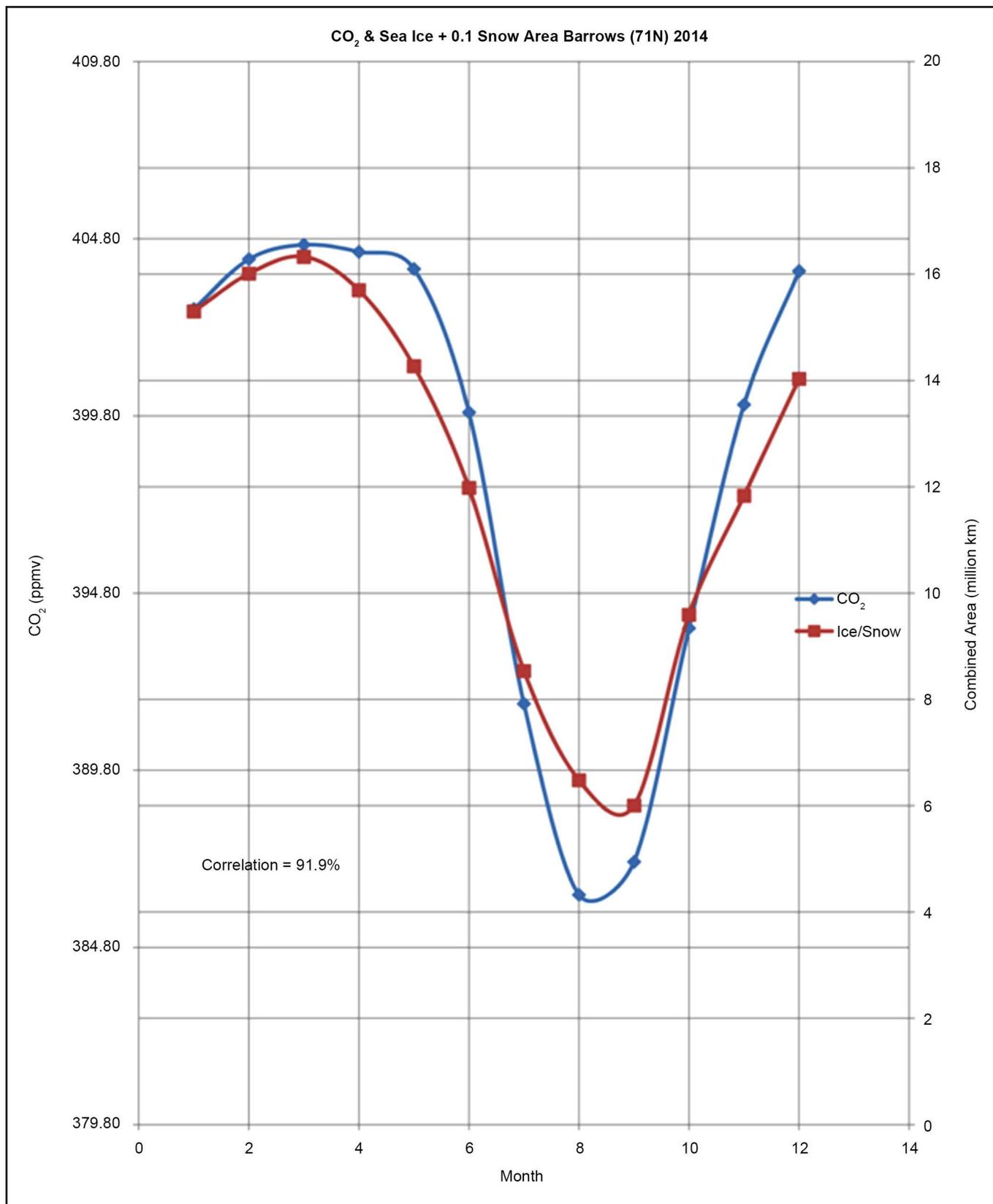
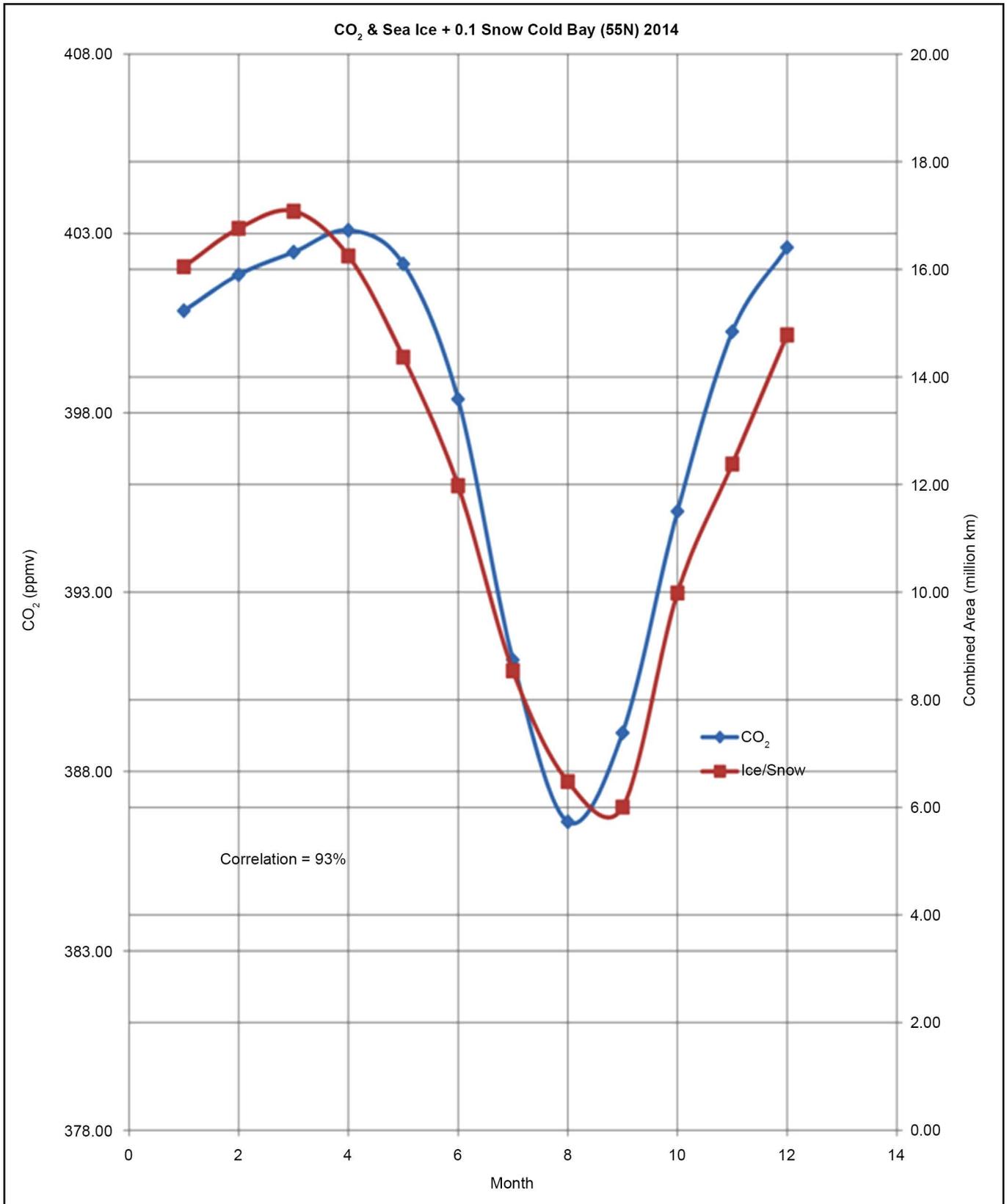**Figure 29.** Plot of CO_2 & sea ice + snow for Barrows, Alaska in 2014. Ice & snow data from NSIDC.

Figure 30. Plot of CO₂ & sea ice + snow for cold bay, Alaska in 2014. Ice & snow data from NSIDC.

than a month. A two week time shift would affect the curves and likely increase the correlation percent. In addition, there are variables that have not been included. The Polar Cell circulates air vertically by lifting the air at 55 - 60 degree latitude and dropping it near the poles.

This would have the effect of accelerating the concentration drop while inhibiting the concentration rise. Incorporating a time lag factor and a wind factor into the curves would likely improve the correlation percent.

Figure 30 (Cold Bay) shows that the freezing process began in September 2014 and continued to December. The melting period started in March and ended in September. The correlation percent was 92%.

Figure 31 and Figure 32 are plots of sea ice and CO_2 for Palmer Station, Antarctica (64˚S) and Ushuaia, Argentina (54.8˚S). These two figures each show high correlations. Palmer Station showed a correlation of 93.6% and Ushuaia, Argentina exhibited an 88.1% correlation. A drop of 4% in correlation could have been caused by the Polar Cell influence. Both stations had similar consistencies in the correlation over the years, as set forth in Table 3.

Each of the stations in the Southern Hemisphere used a sea ice scale of 0 to 25 million square kilometers. A slightly higher sea ice scale was used in the south because of the higher sea ice surface areas. The CO_2 concentration used a scale of 6 ppmv because of the narrower spread. These same scales were used on each of the stations in the SH.

The concentrations may change between stations and between years to reflect the differences, but the same scale was applied to all. The curves were remarkably similar to those in the Northern Hemisphere except the lows and highs were flipped to reflect the season differences. The results were similar with different oceans. Figure 33 is for Iceland (63N) in the Atlantic Ocean in 2014. It showed a correlation percent of 87%. Figure 34 is for Cape Grim in the Indian Ocean with a correlation of 97%. The high correlation at Cape Grim was unexpected since it was believed to be beyond the influence from the polar ice.

Table 3 shows these variations over years. The average correlation for the NH for all of the stations and all years was 91%. The average correlation for the SH was 91%. In order to compare the correlation with different years, a time factor reflecting the yearly increase in CO_2 was applied. This time factor is roughly 0.5%/yr which is the same percent as the CO_2 rise.

The South Pole had a lower correlation (82.7% in 2014) than any of the other stations presented in the table. This was unexpected. One explanation is that the South Pole is located a considerable distance from the freezing sea ice boundary.

In sum, ice (and a small percentage of snow) is the only mechanism that can explain why the CO_2 concentrations are the highest in the Polar Regions; the calculations show that such is capable of causing the 20 ppmv fluctuation in that region; and that the CO_2-Sea Ice curves show a remarkable correlation. It is believed that in the remainder of the world (below 50 degrees in the north and below 40 degrees in the south) the fluctuations are governed by biological and oceanic actions.
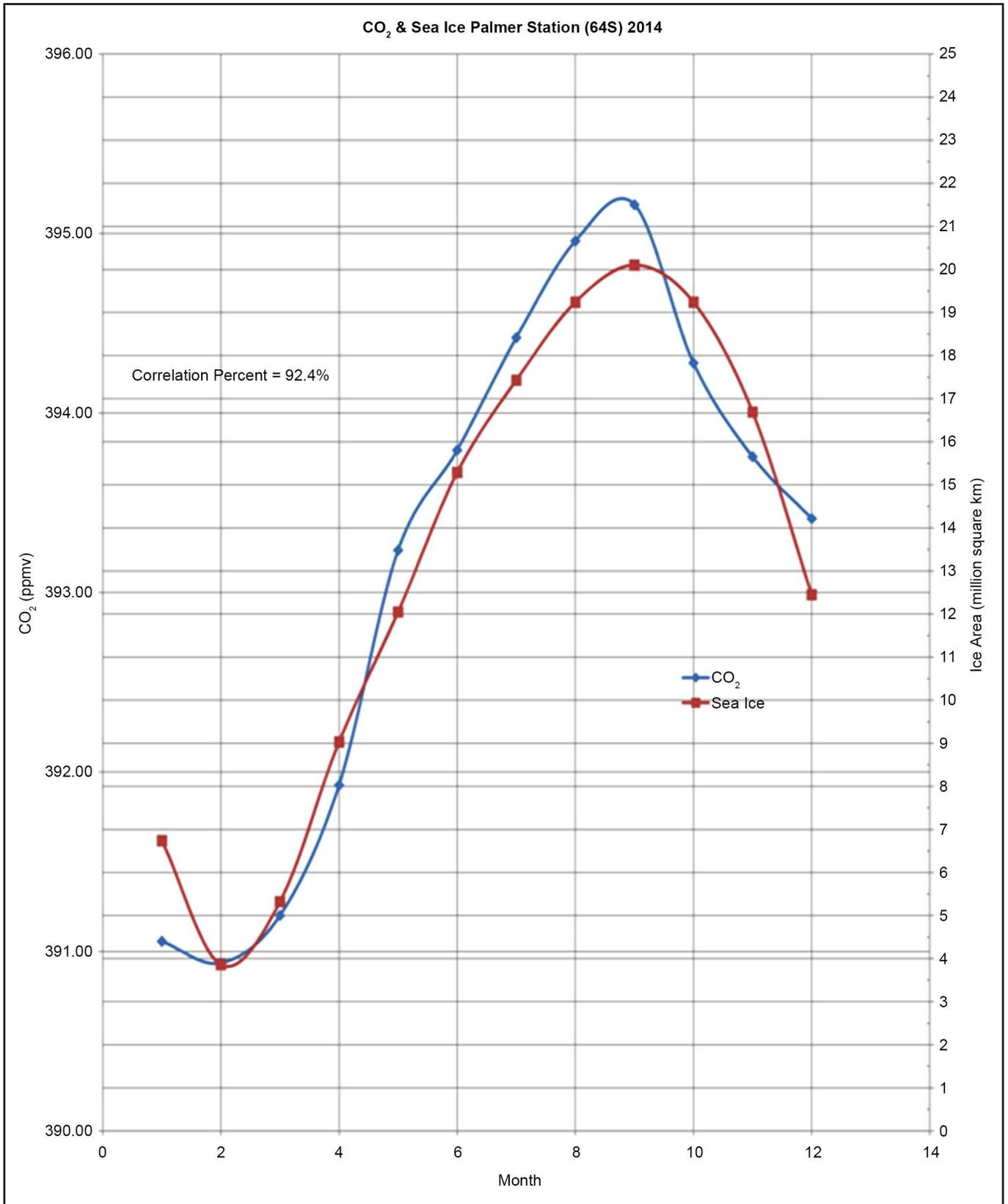
Figure 31. Plot of CO_2 & sea ice for palmer station, Antarctica in 2014. Ice & snow data from NSIDC.
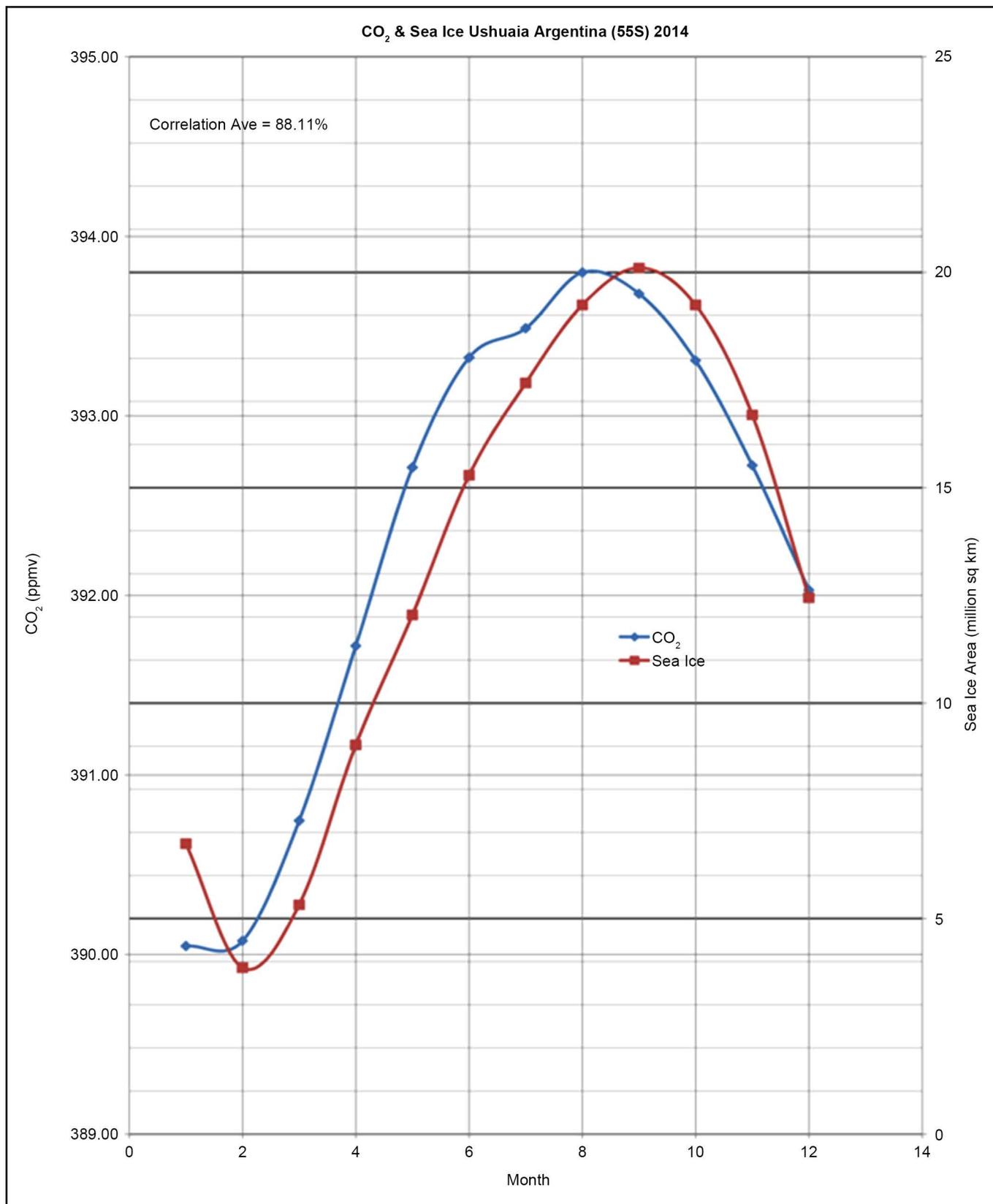
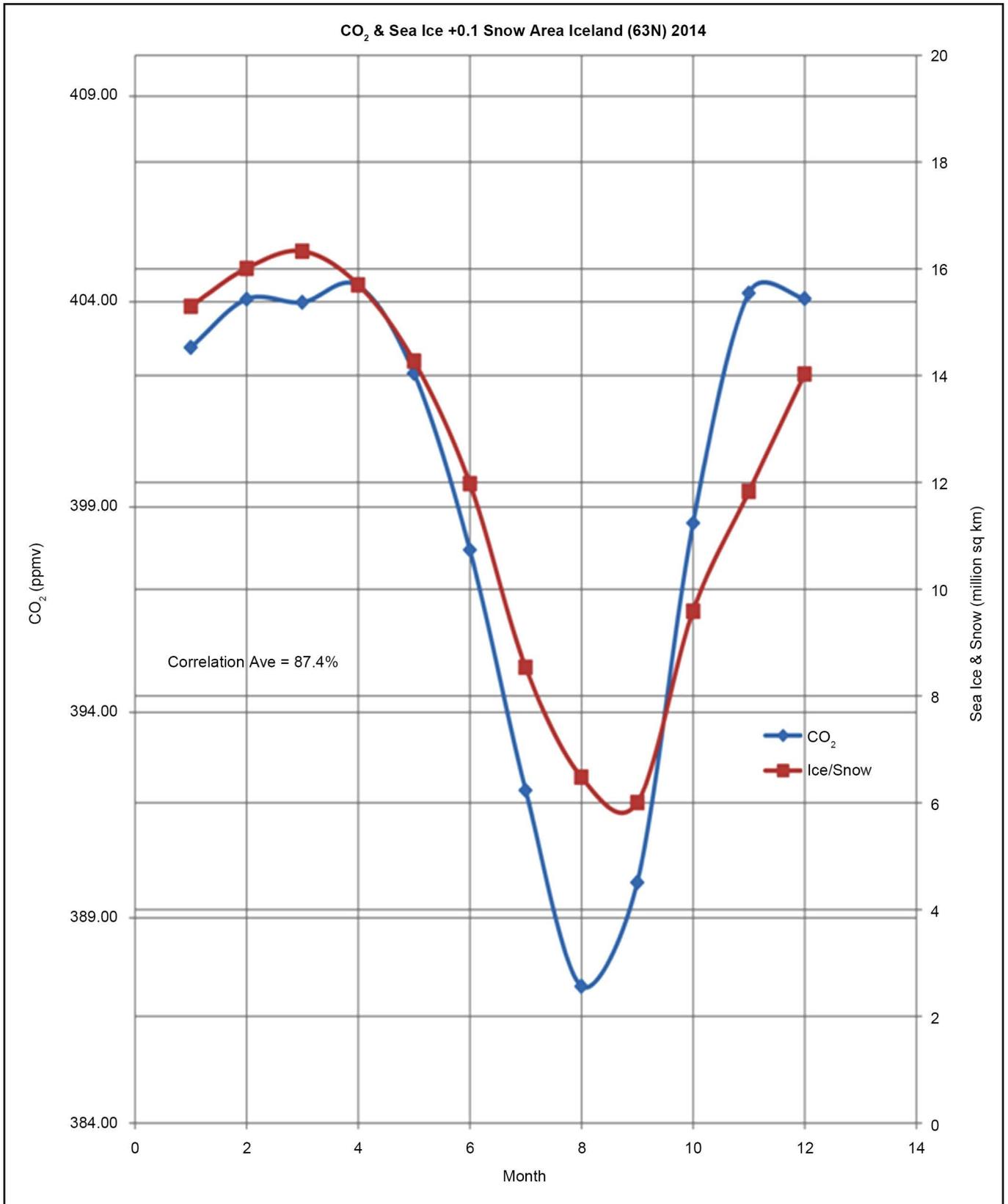**Figure 32.** Plot of CO_2 & sea ice for Ushuaia, Argentina in 2014. Ice data from NSIDC.

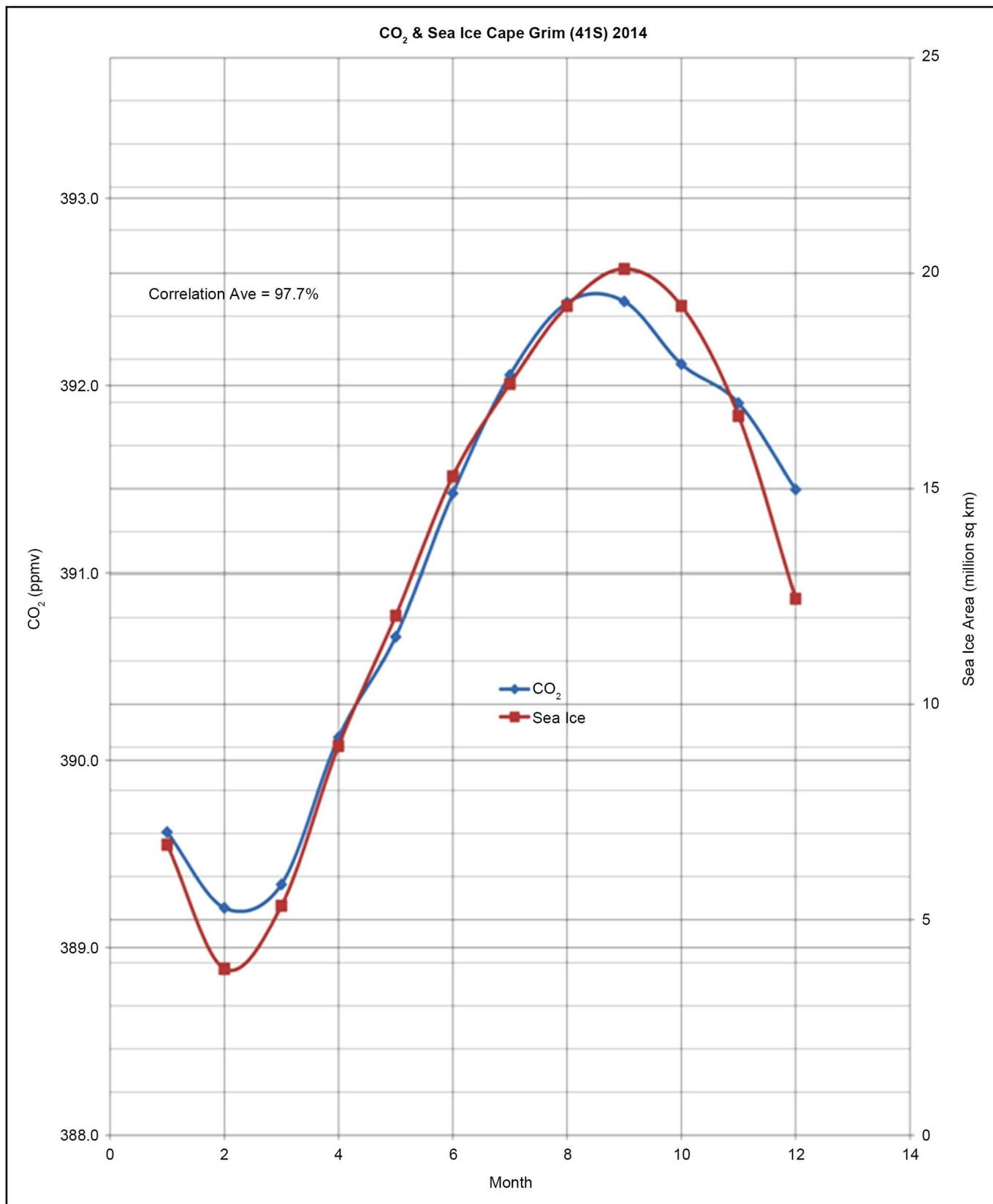**Figure 33.** Plot of CO₂ & sea ice for Iceland in 2014. Ice & snow data from NSIDC.

Figure 34. Plot of CO_2 & sea ice for cape grim, Australia in 2014. Ice data from NSIDC.

Table 3. Correlation percentages on curve relationship between monthly CO_2 concentrations and Sea Ice (and Snow when applicable) for the specified years near the polar areas in both hemispheres. Ice data from NSIDC.

Station	Lat.	Year	Correlation Percent	Ave % Correlation
Northern Hemisphere				
Alert, Canada	82˚N	2014	94.3	
Alert, Canada	82˚N	2011	92.5	
Alert, Canada	82˚N	2007	92.0	
Alert Canada	82˚N	2000	90.7	92.4%
Barrows, Alaska	71˚N	2014	91.9	
Barrows, Alaska	71˚N	2011	84.2	
Barrows, Alaska	71˚N	2007	91.4	
Barrows, Alaska	71˚N	2000	91	89.6%
Iceland	63˚N	2014	87.4	
Iceland	63˚N	2011	90.4	
Iceland	63˚N	2007	92.6	
Iceland	63˚N	2000	91.8	90.6%
Cold Bay, Alaska	55˚N	2014	92.1	
Cold Bay, Alaska	55˚N	2011	86.9	
Cold Bay, Alaska	55˚N	2007	88.8	
Cold Bay, Alaska	55˚N	2001	90.8	89.7%
Southern Hemisphere				
Palmer Station	−64˚S	2014	93.6	
Palmer Station	−64˚S	2011	93.3	
Palmer Station	−64˚S	1997	90.2	92.4
Ushuaia, Argentina	−54.8˚S	2014	88.1	
Ushuaia, Argentina	−54.8˚S	2011	90.4	
Ushuaia, Argentina	−54.8˚S	2007	87.3	88.6
Cape Grim, Australia	−41˚S	2014	97.7	
Cape Grim, Australia	−41˚S	2011	89.6	
Cape Grim, Australia	−41˚S	2005	91.9	
Cape Grim, Australia	−41˚S	2001	92.5	92.9

4. Summary

A Non Dispersive Infrared Analyzer (NDIR) has been used by most testing agencies to measure the atmospheric CO_2 concentrations. This device only works when all of the water vapor is removed. This results in a "dry" value, which can be 10 to 15 ppmv higher than the actual value. The actual concentrations are similar to the dry values but shifted lower with the downward shift becoming larger as the latitude decreases. This downward shift can only be seen with the actual concentrations as anomalies almost entirely mask the difference. This investigation uses actual CO_2 concentrations calculated from the dry values by adding water vapor back into the air using the average monthly specific humidity at each station.

Observations of the CO_2 rise, swing and spread (fluctuations) were measured at many stations over multiple latitudes in both Hemispheres since 1972. Graphical analysis was done comparing CO_2 concentrations with sea temperatures, fossil fuel emissions, humidity, and sea ice and snow. Various assessment techniques were used to interpret the curves and data including: R squared, correlation percent, variability, residence time, absorption percent, etc. The Troposphere effect was considered for short term observations.

Based on the observations and analysis, several conclusions were made on the causes for the CO_2 "rise" (increases each year) and "spread" (seasonal fluctuations).

Several causes for the CO_2 "**rise**" were investigated. The first one addressed was whether an increase in the ocean temperature of 0.7˚F over the last 33 years could have caused the 60 ppmv increase (128 GtC). A curve comparison (**Figure 18**) of CO_2 rise with an integrated ocean temperature showed a correlation of 99.5%. A mass balance calculation showed that the temperature increase could deliver ~200 GtC during that period, which constituted 64% more than needed. The IPCC has shown that out of 197 GtC/yr of CO_2 entering the atmosphere 194 GtC/yr is removed each year. This supports a 98.48% absorption factor. When this absorption factor is applied, the ocean temperature increase would account for only 2.5% of the total CO_2 rise. Fossil fuel emissions were another cause investigated. A curve comparison before (**Figure 19**) and after (**Figure 20**) a 33-year residence time adjustment showed a low correlation. A mass balance calculation showed that the amount of CO_2 emissions could provide 165 GtC during that period and such was 29% more than needed. When the absorption factor is applied, the emissions would account for 1.5% of the total CO_2. Short term observations support a very high absorption factor. These observations include the following: There was no measurable relationship of CO_2 concentration with the US CO_2 emissions (**Figure 25**). The CO_2 percent rise in the Northern Hemisphere was 15.3% and the percent rise in the Southern Hemisphere exhibited the same percent (**Table 2**). This does not support a NH emissions effect, but does corroborate a high absorption rate. An analysis of the Troposphere Effect (**Figure 22**) shows that if 90% of the emissions occurred in the NH between the latitudes of 30N and 60N, then such would increase the CO_2 concentration by 10 to 30 ppmv. This is not supported by observations and validates a very high absorption rate. The other causes/factors that are associated with the remaining

96% of the total rise include: animal biology from land and oceans (particularly bacterial and insect density which are temperature related), land soil moisture changes (temperature related), volcanic events (recent studies show CO_2 emissions much higher than previously believed), and uncertainties and errors in the derivation of the carbon cycle numbers.

Various causes for the CO_2 "**spread**" (seasonal fluctuations) were investigated. The most important cause from a global standpoint is associated with biology. This has been the subject of many scientific studies as being the predominate cause for the seasonal CO_2 fluctuations. This investigation agrees with those studies. However, other potential causes were considered.

Plots of sea temperature changes with CO_2 concentrations showed that there was a very high inverse correlation. That is, as the temperature went up, the short term concentration went down and vice versa. This inverse relationship negates sea temperatures as the direct cause. However, it could be acting as a proxy. The types of proxy relationships include marine biology, *i.e.* as sea temperatures rise, phytoplankton activity increases, which causes the CO_2 concentration to decline. Another proxy relationship may be rain. Rain increases with increasing temperature & humidity. The more rain, the more CO_2 is scrubbed from the atmosphere, causing the CO_2 concentration to drop. In addition to a proxy explanation, a six month delay between sea temperature and CO_2 changes could make the two consistent. This study did not find nor investigate observational evidence to support either a proxy or a six month delay time. Based on all of these factors, a connection between changing sea temperatures and CO_2 seasonal fluctuations remains uncertain.

Graphical analysis between CO_2 and US fossil fuel emissions from observation stations north, south and to the west of the United States did not show a detectible connection. The Troposphere Effect coupled with actual observations negates a relationship. The fact that the NH changed at the same percentage as the SH, does not support a connection. And the lack of scientific studies connecting CO_2 emissions to the seasonal fluctuations supports the conclusion that fossil fuel emissions do not cause or contribute, in any measurable way, to seasonal fluctuations. None of the potential causes discussed above provided any explanation as to why the Polar Regions have the highest CO_2 concentrations.

When sea ice freezes, it ejects all of the CO_2 that is contained in the water. Mathematical computations confirm that the CO_2 ejected from the changes in sea ice volume was sufficient to cause a 20 degree fluctuation in the CO_2 concentration in the Polar Circles. Graphical analysis at several different latitudes in the polar and near Polar Regions, for multiple years, showed a 90% correlation. Sea ice also provides a reasonable explanation as to why the highest concentration of CO_2 occurs in the Polar Area. The remainder of the world (below 50 degrees in the north and below 40 degrees in the south) the fluctuations are believed to be controlled primarily by biological actions.

References

[1]   IPCC (1990) 1st Assessment Report, WG1. Cambridge University Press, Cambridge.

[2] Soares, P.C. (2010) Warming Power of CO_2 and H_2O: Correlations with Temperature Changes. *International Journal of Geosciences*, **1**, 102-112. http://dx.doi.org/10.4236/ijg.2010.13014

[3] Buermann, W., Lintner, B.R., Koven, C.D., Angert, A., Pinzon, J.E., *et al.* (2007) The Changing Carbon Cycle at Mauna Loa Observatory. *Proceedings of the National Academy of Sciences of the United States of America,* **104**, 4249-4254. http://dx.doi.org/10.1073/pnas.0611224104

[4] Keeling, C., Chin, J. and Whorf, T. (1996) Increased Activity of Northern Vegetation Inferred from Atmospheric CO_2 Measurements. *Nature,* **382**, 146-149. http://dx.doi.org/10.1038/382146a0

[5] Keeling, R. (2008) Recording Earth's Vital Signs. *Science*, **319**, 1711-1712. http://dx.doi.org/10.1126/science.1156761

[6] Schaefer, K., Denning, S. and Owen, L. (2005) The Winter Arctic Oscillation, the Timing of Spring, and Carbon Fluxes in the Northern Hemisphere. *Global Biogeochemical Cycles*, **19**, Article ID: GB3017.

[7] Denning, S., Fung, I. and Randall, D. (1995) Latitudinal Gradient of Atmospheric CO_2 Due to Seasonal Exchange with Land Biota. *Nature,* **376**, 240-243. http://dx.doi.org/10.1038/376240a0

[8] Zhou, Z., Xu, M., Kang, F. and Sun, O.J. (2015) Maximum Temperature Accounts for Annual Soil CO_2 Efflux in Temperate Forests of Northern China. *Scientific Reports*, **5**, Article ID: 12142. http://dx.doi.org/10.1038/srep12142

[9] Du, E., Zhou, Z., Peng, L., Yiang, L., Hu, X. and Fang, J. (2013) Winter Soil Respiration during Soil Freezing Process in a Boreal Forest in Northeast China. *Journal of Plant Ecology*, **10**, Article ID: 1093.

[10] McGuire, A.D., Christensen, T.R., Hayes, D., Heroult, A., Euskirchen, E., *et al.* (2012) An Assessment of the Carbon Balance of Arctic Tundra: Comparisons among Observations, Process Models, and Atmospheric Inversions. *Biogeosciences*, **9**, 3185-3204. http://dx.doi.org/10.5194/bg-9-3185-2012

[11] Jiang, X., Chahine, M., Li, Q., Liang, M., Olsen, E., *et al.* (2012) CO_2 Semiannual Oscillation in the Middle Troposphere and at the Surface. *Global Biogeochemical Cycles,* **26**, Article ID: GB3006.

[12] Trabalka, J.R. (1985) Atmospheric Carbon Dioxide and the Global Carbon Cycle. US Department of Energy Oak Ridge National Laboratory, DOE/ER 0239.

[13] Reichenau, T. and Esser, G. (2003) Is Interannual Fluctuation of Atmospheric CO_2 Dominated by Combined Effects of ENSO and Volcanic Aerosols? *Global Biogeochemical Cycles,* **17**, Article ID: 1094.

[14] Verdy, A., Dutkiewicz, S., Follows, M.J., Marshall, J. and Czaja, A. (2007) Carbon Dioxide and Oxygen Fluxes in the Southern Ocean: Mechanisms of Interannual Variability. *Global Biogeochemical Cycles,* **21**. http://dx.doi.org/10.1029/2006GB002916

[15] Dettinger, M.D. and Ghil, M. (1998) Seasonal and Interannual Variations of Atmospheric CO_2 and Climate. *Tellus,* **50B**, 1-24.

[16] Stephens, B.B., Keeling, R., Heimann, M., Six, K.S., Murnane, R. and Caldeira, K. (1998) Testing Global Ocean Carbon Cycle Models Using Measurements of Atmospheric and Concentrations of Atmospheric O_2 and CO_2 Concentration. *Global Biogeochemical Cycles,* **12**, 213-230.

[17] Thoning, K.W., Conway, T.J., Zhang, N. and Kitzis, D. (1995) Analysis System for Measurement of CO_2 Mixing Ratios in Flask Air Samples. *Journal of Atmospheric and Oceanic*

Technology, **12**, 1349-1356.
http://dx.doi.org/10.1175/1520-0426(1995)012<1349:ASFMOC>2.0.CO;2

[18] Blunden, J. and Arndt, D. (2014) State of the Climate in 2013. *Bulletin of the American Meteorological Society*, **95**, S1-S257.
http://dx.doi.org/10.1175/2014BAMSStateoftheClimate.1

[19] Sonnemann, G.R. and Grygalashvyly, M. (2013) Effective CO_2 Lifetime and Future CO_2 Levels Based on Fit Function. *Annales Geophysicae*, **31**, 1591-1596.
http://dx.doi.org/10.5194/angeo-31-1591-2013

[20] Jacobson, M.Z. (2005) Correction to "Control of Fossil-Fuel Particulate Black Carbon and Organic Matter, Possibly the Most Effective Method of Slowing Global Warming". *Journal of Geophysical Research*: *Atmospheres*, **110**, 4105. http://dx.doi.org/10.1029/2005JD005888

[21] Dietze, P. (1995) Bei konstanter CO_2-Emission keine Klimakatastrophe, Ein neues globales Kohlenstoffmodell, Europäische Akademiefür Umweltfragen, Leipzig, conference papers.

[22] Kikuchi, R., Gorbacheva, T. and Gerardo, R. (2009) Reconsideration of Atmospheric CO_2 Lifetime: Potential Mechanism for Explaining CO_2 Missing Sink. *Geophysical Research Abstracts*, **11**, EGU2009-3381.

[23] Andrews, R. (2014) The Residence Time of CO_2 in the Atmosphere is 33 Years? Blog on Energy, Environment and Policy.
http://euanmearns.com/the-residence-time-of-co2-in-the-atmosphere-is-33-years/

[24] Conover J PE, New York, (2011) Referencing wikipedia.org
http://www.jconoverjr.com/html/global_warming__and_the_oceans.html

[25] Broecker, W. (1974) Chemical Oceaneanography. Harcourt Brace Jovanovich Inc., San Diego, CA.

[26] Wikipeda (2016) Oceans. https://en.wikipedia.org/wiki/Ocean

[27] Wikipeda (2016) Biomass. https://en.wikipedia.org/wiki/Biomass_(ecology)

[28] Wikipeda (2016) Soil Respiration. https://en.wikipedia.org/wiki/Soil_respiration

[29] Burton, M.R., Sawyer, G. and Granieri, D. (2013) Deep Carbon Emissions from Volcanoes, *Reviews in Mineralogy & Geochemistry*, **75**, 323-354.
http://dx.doi.org/10.2138/rmg.2013.75.11

[30] Orange, R. (2013) Volcanic Range Discovered off Norway, News Publication.
http://www.thelocal.no/20130802/Volcanic-range-discovered-in-Norwegian-waters

[31] Wang, Y.P., Baldocchi, D., Leuning, R., Falges, E. and Vesala, T. (2007) Estimating Parameters in a Land-Surface Model by Applying Nonlinear Inversion to Eddy Covariance Flux Measurements from Eight FLUXNET Sites. *Global Change Biology*, **13**, 652-670.
http://dx.doi.org/10.1111/j.1365-2486.2006.01225.x

[32] Myneni, R.B. and Asrar, G. (1994) Atmospheric Effects and Spectral Vegetation Indices. *Remote Sensing of Environment*, **47**, 390-402.

[33] Official Data, NASA 2002 Earth Observatory Global Maps.
http://earthobservatory.nasa.gov/GlobalMaps/view.php?d1=TRMM_3B43M&d2=AMSRE_SSTAn_M

[34] Papadimitriou, S., Kennedy, H., Kattner, G., Dieckmann, G.S. and Thomas, D.N. (2003) Experimental Evidence for Carbonate Precipitation and CO_2 Degassing during Sea Ice Formation, Pergamon. *Geochimica et Cosmochimica Acta*, **68**, 1749-1761.

[35] Rysgaard, S., Glud, R.N., Sejr, M.K., Bendtsen, J. and Christensen, P.B. (2007) Inorganic Carbon Transport during Sea Ice Growth and Decay: A Carbon Pump in Polar Seas. *Journal of Geophysical Research*: *Oceans*, **112**, C03016. http://dx.doi.org/10.1029/2006jc003572

[36] Loose, B., McGillis, W.R., Schlosser, P., Perovich, D. and Takahashi, T. (2009) Effects of Freezing, Growth, and Ice Cover on Gas Transport Processes in Laboratory Seawater Experiments. *Geophysical Research Letters*, **36**, Article ID: LO5603.

[37] Geilfus, N.X., Tison, J.L., Ackely, S.F., Galley, R.J., Rysgaard, S., *et al.* (2014) Sea Ice pCO$_2$ Dynamics and Air-Ice CO$_2$ Fluxes during the Sea Ice Mass Balance in the Antarctic (SIMBA) experiment-Bellingshausen Sea, Antarctica. *The Cryosphere,* **8**, 2395-2407. http://dx.doi.org/10.5194/tc-8-2395-2014

[38] Geilfus, N.X., Carnat, G., Papkyriakou, T., Tison, J.L., Else, B., *et al.* (2012) Dynamics of pCO$_2$ and Related Air-Ice CO$_2$ Fluxes in the Arcticcoastal Zone (Amundsen Gulf, Beaufort Sea). *Journal of Geophysical Research,* **117**, Article ID: COOG10.